3% (see Figure 16). One of these SVs was an inversion of 2p arm which co-occurred with MYCN amplification, and was thus not considered as novel but a result of the formation of DMs involving this locus[39]. Of note, these variants were almost absent in the intermediate to low-risk tumors (only 3 low risk tumors from EGA dataset had t(4p-17q). $P_{TARGET} = 8\times10^{-11}$; $P_{EGA} = 4.40\times10^{-7}$), and occurred alone or in combination with other recurrent SVs (Figure 38).

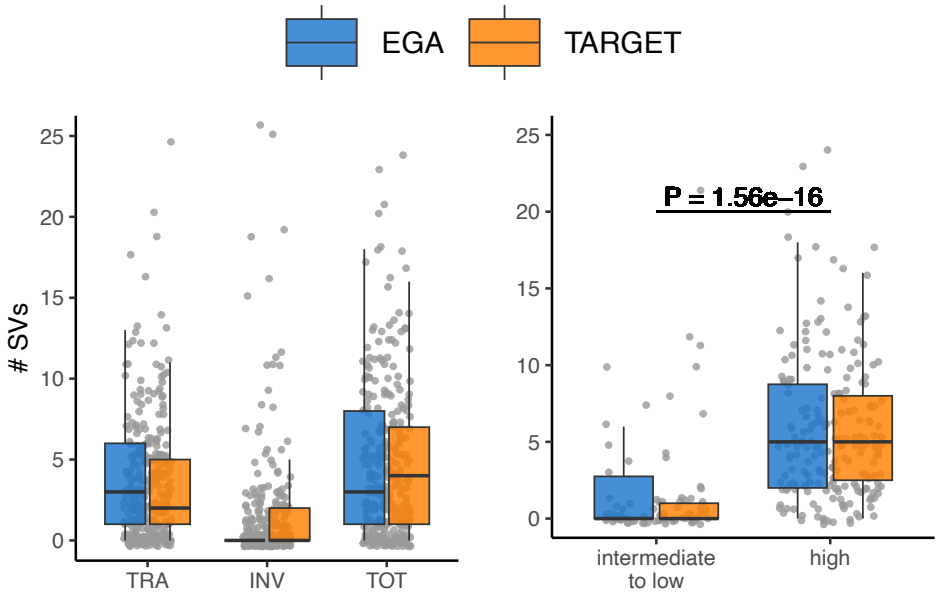

Figure 34. Distribution of SVs across NBL datasets and risk groups.

Box plots on the left show the distribution of translocations (TRA), inversions (INV) and all the SVs (TOT) across EGA and TARGET samples, while those on the left the distribution of SVs between risk groups. P-value derived from a Mann Whitney U test.

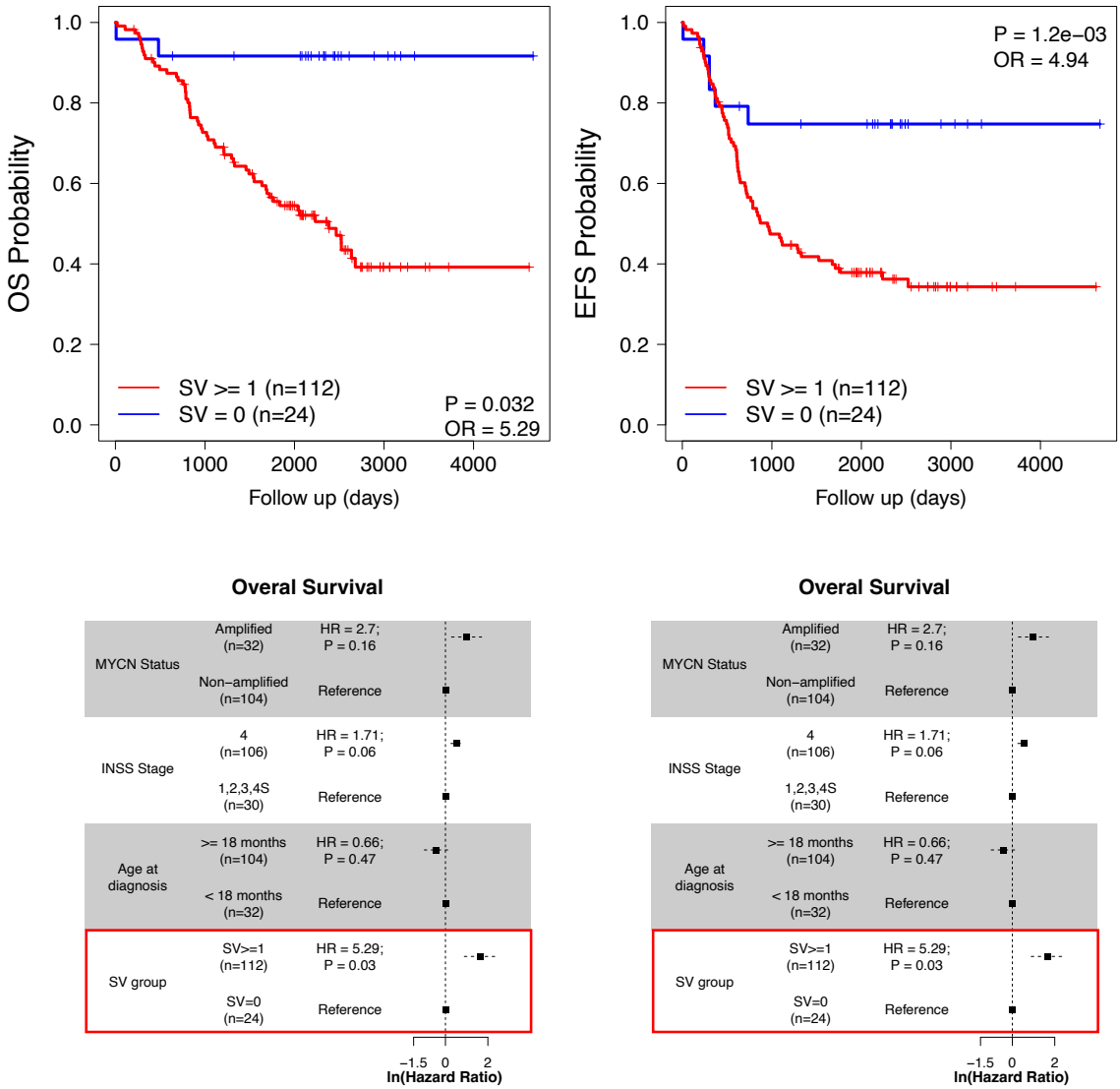

Figure 35. The presence of at least an SV predicted less overall survival in a multivariate Cox proportioned hazard regression model in TARGET dataset.

Kaplan-Meier curves (top) the OS (top-left) and the EFS (top-right) probability of TARGET samples divided in two groups according the presence (red line) or the absence (blue line) of at least an SV in a univariate model, while the tables below show the results of a multivariate Cox proportioned-hazard regression model adjusting for *MYCN* status, INSS stage and the age at diagnosis. Squared dots and dashed lines represent the estimates and the standard errors, respectively. Red box highlights the contribution of the presence at least an SV (SV>=1) to the OS (bottom-left) and EFS (bottom-right) probability in this model.

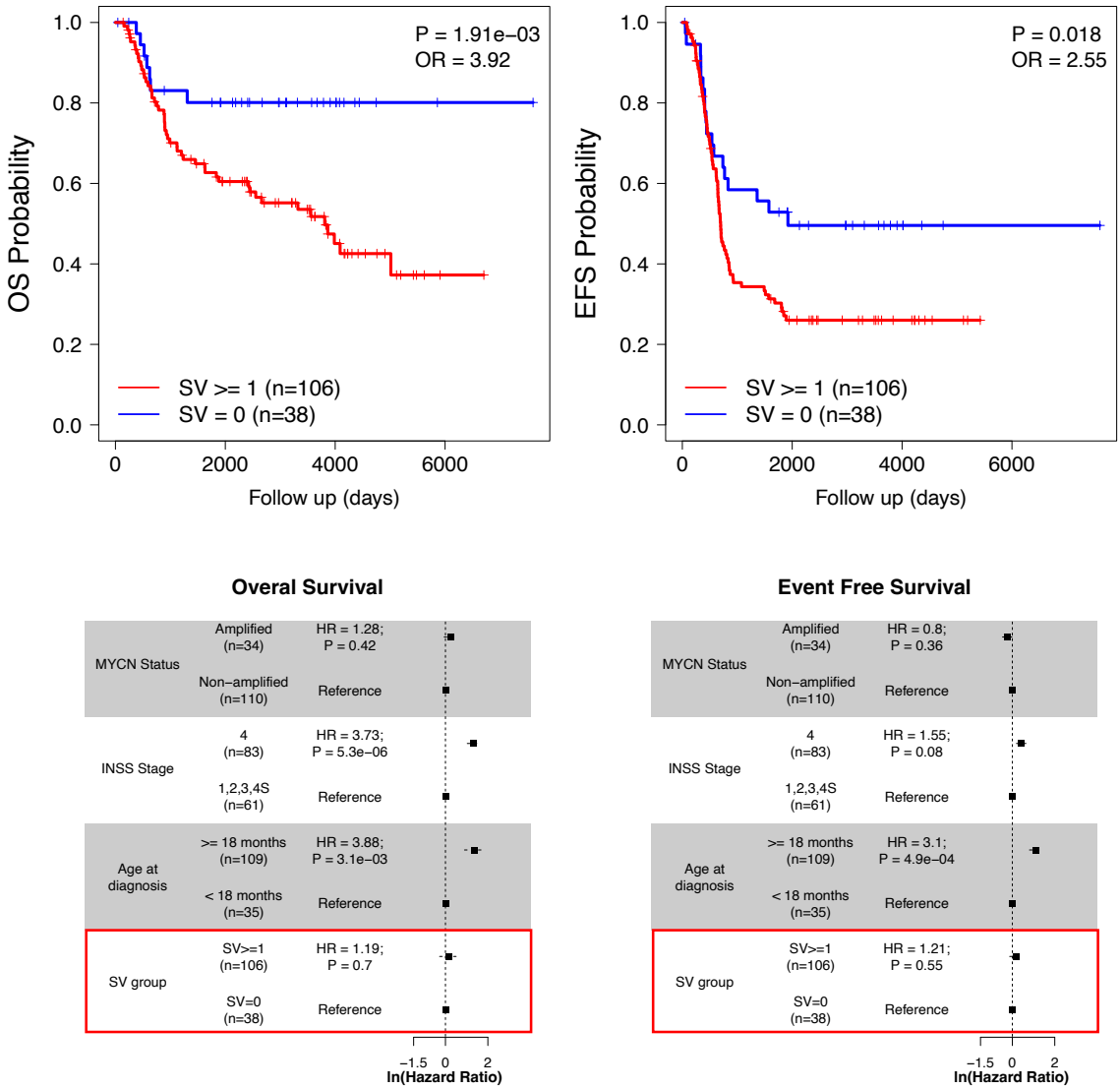

Figure 36.The presence of at least an SV predicted less overall survival in a univariate model in EGA dataset.

Kaplan-Meier curves (top) the OS (top-left) and the EFS (top-right) probability of EGA samples divided in two groups according the presence (red line) or the absence (blue line) of at least an SV in a univariate model, while the tables below show the results of a multivariate Cox proportioned-hazard regression model adjusting for *MYCN* status, INSS stage and the age at diagnosis. Squared dots and dashed lines represent the estimates and the standard errors, respectively. Red box highlights the contribution of the presence at least an SV (SV>=1) to the OS (bottom-left) and EFS (bottom-right) probability in this model.

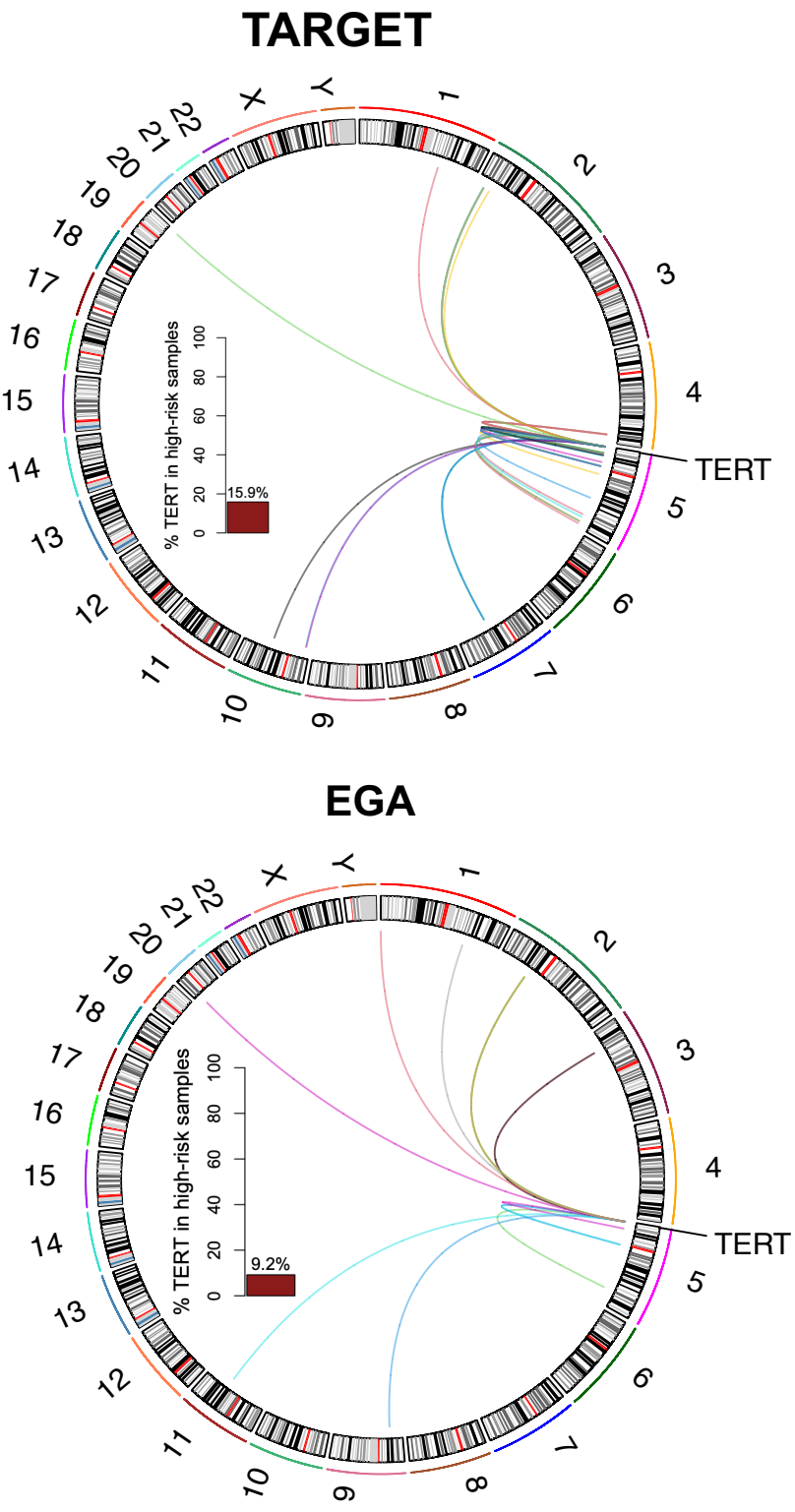

Figure 37. TERT rearrangements in NBL samples.

Circos plot showing the rearrangements (inversions and translocations) in *TERT* region – defined as 300Kb upstream and downstream the gene locus – in TARGET (top) and EGA (bottom) samples. The inner bar plot shows the frequency of rearrangements in high-risk group.

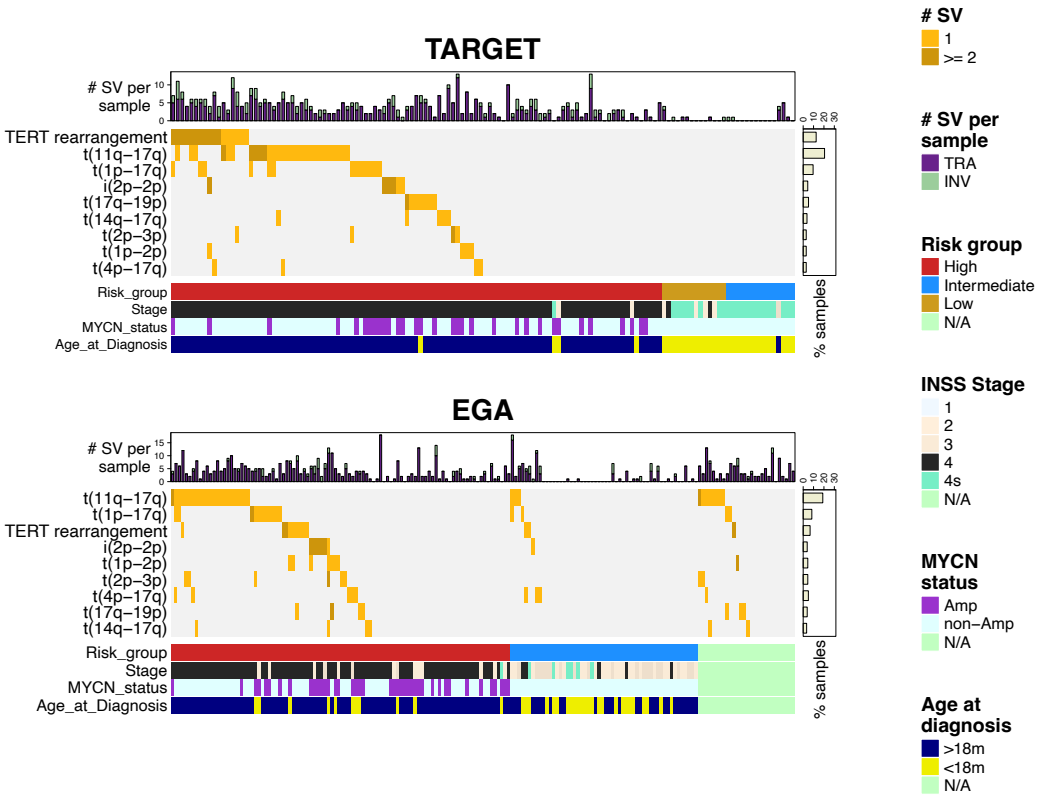

Figure 38. Recurrent SVs in NBL.

Heatmaps showing the occurrence of the most common (≥ 4 and ≥ 6 samples affected in TARGET and EGA dataset, respectively) SVs (rows) in TARGET (bottom) and EGA (bottom) samples (columns), alongside with samples annotations – regarding clinical parameters (bottom annotation) and number of SVs (top annotation) – and frequency of each SV (right annotation).

Collectively, breakpoints of these 6 SVs overlapped with the gene-body of 80 and 91 protein-coding genes of TARGET and EGA samples, respectively, putatively leading to the LoF of these genes. Of these, a total of 12 genes was shared between the two datasets (Figure 39).

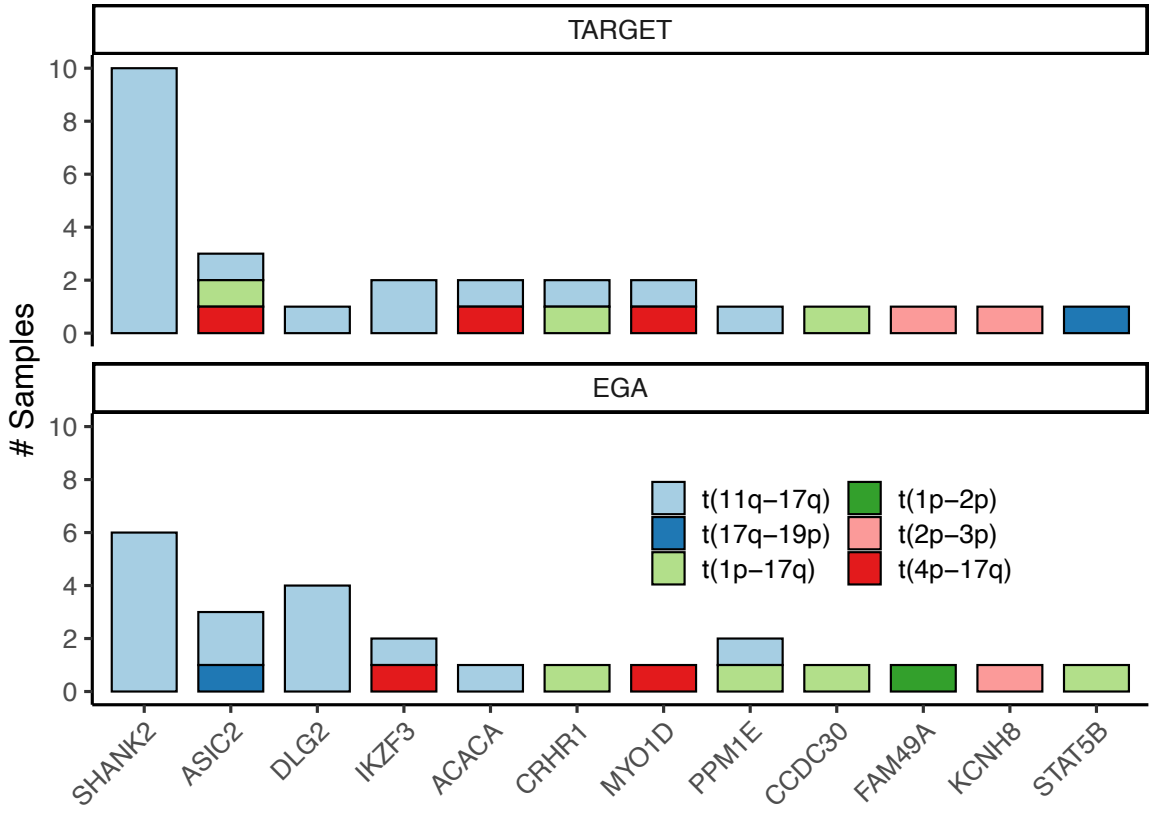

Figure 39. Genes hit by recurrent SVs.

Bar plot showing the number of samples with recurrent SVs (shown in figure legend) affecting 12 genes listed in x-axis in TARGET (top) and EGA datasets (bottom). Bars are colored based on SVs.

In line with literature, the most of these genes have a role in synapse plasticity during the neurodevelopment, and are involved in different neurological and psychiatric diseases[88]. As expected, *SHANK2* was the most frequent gene (10 and 6 samples in TARGET and EGA samples, respectively) disrupted by an SV – the t(11q-17q). It is a known NBL TSG whose expression is decreased in high-risk tumors[88]. Its gene product is a scaffolding protein important for the synapse formation of glutamatergic neurons[187,188]. The same study that identified *SHANK2* as a TSG in NBL also described *DLG2* as frequently hit by breakpoints[88]. We found 5 samples (1 for TARGET and 4 for EGA) in which the t(11q-17q) affected this gene. Similarly to *SHANK2*, *DLG2* encodes a postsynaptic scaffolding protein that interacts with cytoskeleton and glutamatergic NMDA receptors[189]. As *SHANK2*, it is associated to a series of psychiatric and neurological disorders, including schizophrenia, autism spectrum and Parkinson's disease, among the others[190]. However, unlike *SHANK2*, SVs involving *DLG2* alterations are not exclusive of NBL, but are shared in other pediatric malignancies[88,191]. Another interesting gene recurrently disrupted by SVs was *ASIC2*, which was detected in 6 samples (3 EGA and 3 TARGET). *ASIC2* gene product is an acid-sensitive ion channel which is ubiquitously expressed in neurons[192], where it has been proposed to withstand synaptic plasticity[193]. Given its ubiquitous presence in nervous system, it is associated to a large plethora of diseases, ranging from migraine to multiple sclerosis[194]. Although its role in cancer is yet to be defined, it has been shown to promote invasion in an *in vitro* model of colorectal cancer, suggesting a putative role of oncogene[195]. 4 samples (2 EGA and 2 TARGET) carried SVs affecting *IKZF3.* In central nervous system, this gene is expressed by microglia, serving as a modulator of neuroinflammation upon cerebral ischemia[196]. Interestingly, its expression is correlated to positive outcome in melanoma[197] – a tumor that shares embryonal origin with NBL[198] – suggesting a potential role of TSG.

4.3. *NBL patients showed different phenotypes based on the presence of an SV*

As reported in the previous paragraph, the presence of at least an SV predicted OS and EFS probability in NBL samples, and was characteristic of high-risk subtypes (see Figures 34, 35 and 36). To better dissect the implications of the occurrence of SVs in NBL, we divided samples according to the presence or the of at least an SV. For simplicity, we labelled as SV group and as no-SV group samples with at least o no SVs, respectively. We then assessed biological and phenotypical differences between these two groups. In detail, we compared the degree of genetic and genomic instability of these two groups, assessed the SNVs mutational patterns through a mutational signature analysis and evaluated differences in gene-expression profile via DGE analysis using RNA-seq data. Finally, in order to detect a

putative contribution of constitutional genetic variation, we tested germline SNVs for differences between these two groups of samples.

4.3.1. SV group showed an overall increased degree of genetic instability compared to no-SV group

As extensively discussed in *Introduction*, genetic instability – defined as the tendency of a tumor to acquire mutations[199] – is generally considered a marker of poor prognosis in NBL[19,88,166,178]. We thus wanted to assess differences in the extent of genome instability in SV versus no-SV group. To this end, we compared the distribution of 5 parameters as a proxy of genome instability (TMB, number of focal CNAs, number of numerical CNAs, large state transitions and SV burden)[88,147,200] in the two group of samples (Figure 40). 3 out of 5 parameters (TMB, number of focal CNAs and SV burden) were significantly increased in SV group in both datasets (two-sided Mann Whitney's U-test p-value < 5×10^{-7}). LST – defined as the number of CN status variations between segments of at least 5MB[147] (see *Methods*) – were significantly increased in SV group in TARGET (Mann-Whitney U test P = 2.67×10^{-3}) but not in EGA samples (P = 0.179). Interestingly, the number of numerical CNAs was significantly increased in no-SV group in EGA samples (P = 4.32×10^{-4}), although it resulted unvaried in TARGET cohort (P = 0.387). In conclusion, these results suggest that tumors carrying at least an SV are characterized by an increased degree of genetic instability.

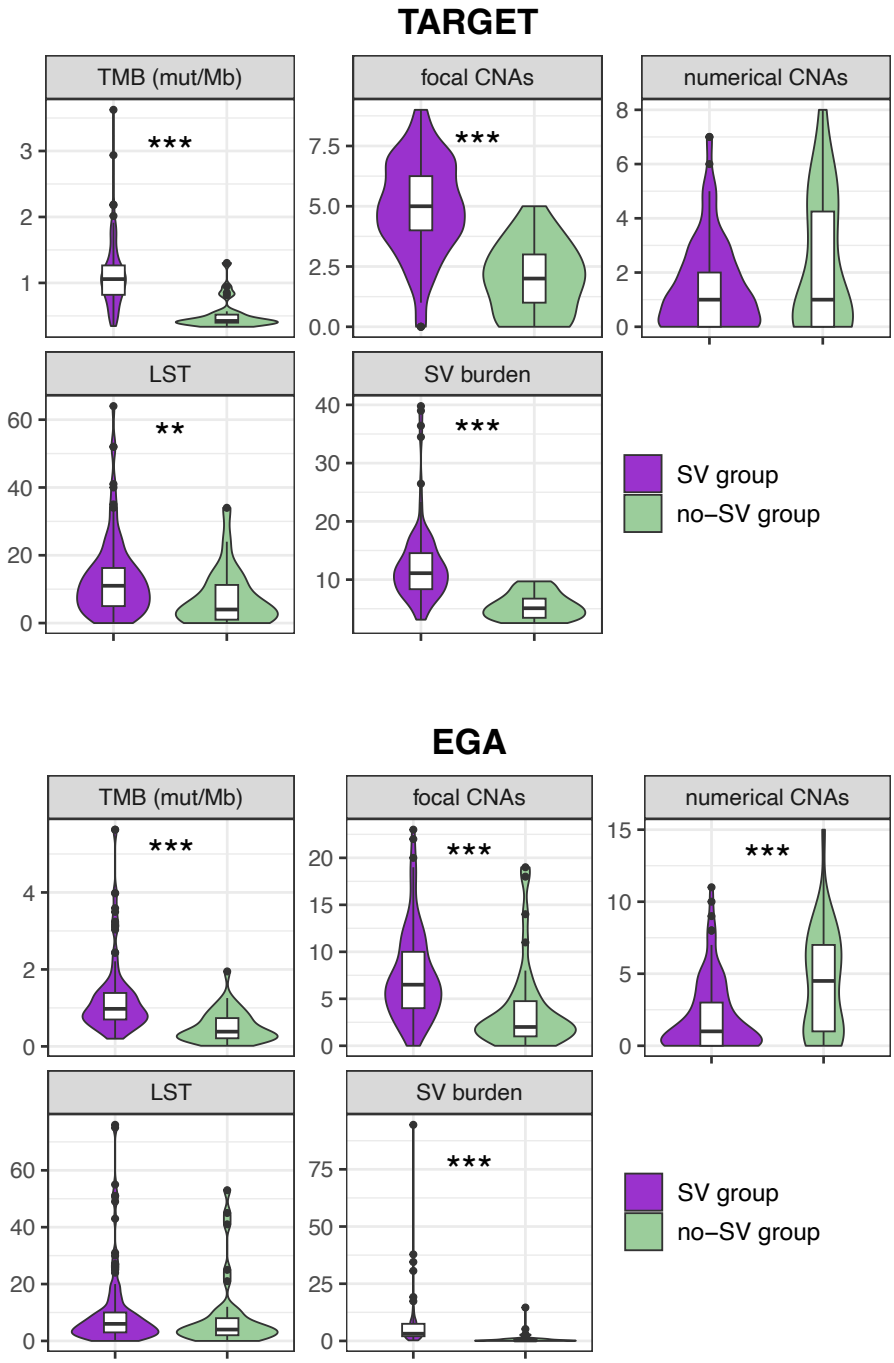

Figure 40. Genome instability is increased in SV group.

Violin plots showing the distribution of 5 genome instability parameters (clockwise: TMB, focal CNAs numerical CNAs, SV burden and LST) across SV and no-SV group in TARGET (top) and EGA (bottom) NBL samples. ***: $P \leq 0.001$; **: $P \leq 0.0$. Statistical significance was assessed through a two-sided Mann Whitney's U-test.

4.3.2. SV group was enriched in mutations of SBS18

WGS-based studies revealed that NBL shows specific mutational patterns[92,93]. Regarding SNVs profiles, it has been described that NBL is characterized by mutational activities ascribable by defined SBSs, which include SBS1, SBS5 and SBS18[92,93,152]. SBS mutational signature analysis performed on somatic SNVs detected activities from 10 Cosmic SBS (Table 5). 4 of these (SBS1, 5, 18 and 40) was shared between the cohorts and found to be active in NBL across more studies[92,93,152].

Signature	EGA samples with signature†	TARGET samples with signature†	Proposed etiology	Reference
SBS1*	**40.00%**	**46%**	**Clock-like (cell division rate)**	***Nik-Zainal et al., 2012***[94]
SBS4	N/A	13.24%	Tobacco smoking	*Alexandrov et al., 2013*[91]
SBS5*	**89.44%**	**98.53%**	**Unknown (probably clock - like)**	***Alexandrov et al., 2013***[91]
SBS18*	**77.22%**	**60.29%**	**Damage by ROS**	***Alexandrov et al., 2013***[91]
SBS38	11.11%	N/A	Indirect effect of UV-light	*Alexandrov et al., 2020*[149]
SBS40*	**52.78%**	**17.64%**	**Unknown**	
SBS51	5.56%	N/A	Possible sequencing artifacts	*Alexandrov et al., 2020*[149]
SBS58	13.33%	N/A	Possible sequencing artifacts	*Alexandrov et al., 2020*[149]
SBS60	10.56%	N/A	Possible sequencing artifacts	*Alexandrov et al., 2020*[149]
SBS96d	N/A	36.02%	Unknown	*Degasperi et al., 2022*[201]

Table 5. SBS signatures active in TARGET and EGA tumors.

*SBSs shared between dataset are shown in bold.

†We considered as active only SBSs with ≥ 5% mutations per sample (see *Methods*).

In both the cohorts, the relative activity – expressed as mutations of a signature in a group divided the total of mutations (see *Methods*) – of SBS1 and SBS5 was increased in the no-SV group, conversely to the relative activity of SBS18 that was higher in the SV group (Figure 41). However, when we considered the absolute number of mutations of each signature, the SBS18 was the only signature that was significantly enriched in the SV group in both datasets ($P < 10^{-4}$) (Figure 42), indicating that the increase of the mutational burden in this group with respect to the no-SV group (see Figure 40) was mainly due to mutations ascribable to this signature. Is known that in NBL the SBS18 correlates with *MYCN* amplification, 17q gain and the expression of mitochondrial genes[152]. To rule out that the difference of SBS18 activity between SV and no-SV group was influenced by these factors, we performed a multivariate logistic regression evaluating the differential distribution of SBS18 activity in SV and no-SV group including the 17q gain, the *MYCN* amplification and

the mitochondrial gene expression as covariates (Figure 43). We observed that SV group was enriched in SBS18 mutation even in presence of covariates (multivariate logistic regression $P < 0.01$), suggesting that the presence of SVs can *per se* induce the activity of this signature.

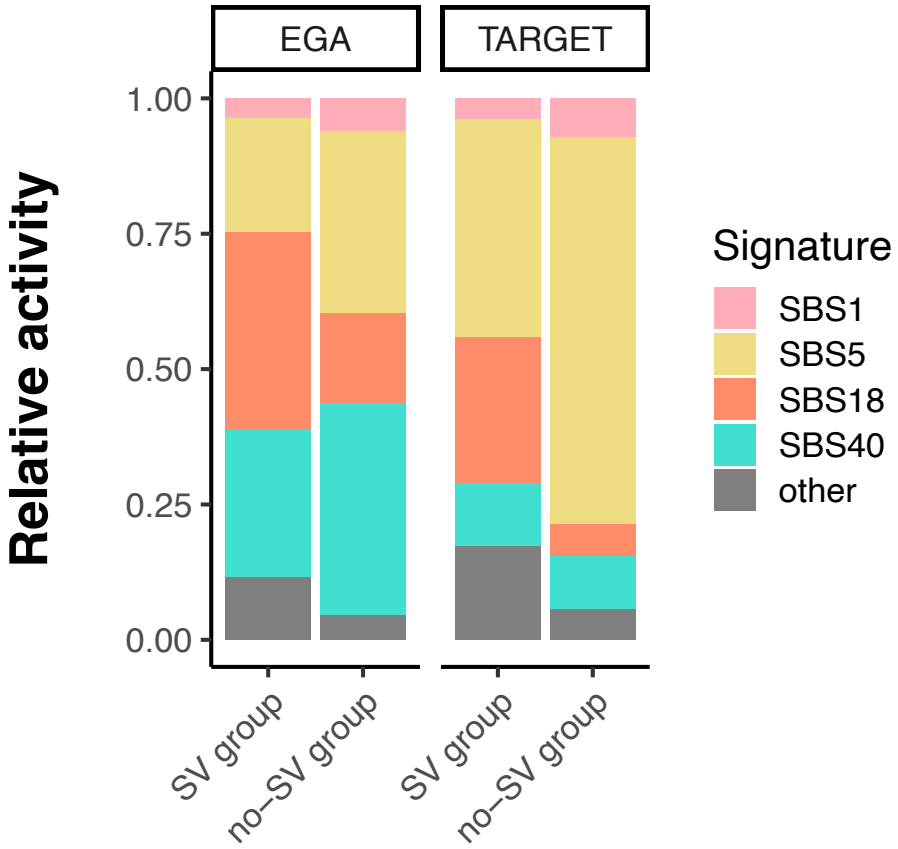

Figure 41. Relative activity of SBS signature in SV and no-SV group.

Stacked bar plot showing the relative activity – expressed as mutations of a signature in a group divided the total of mutations (see *Methods*) – of each of the 4 shared signatures (SBS1, SBS5, SBS18, SBS40) in SV and no-SV group in the two cohorts of NBL.

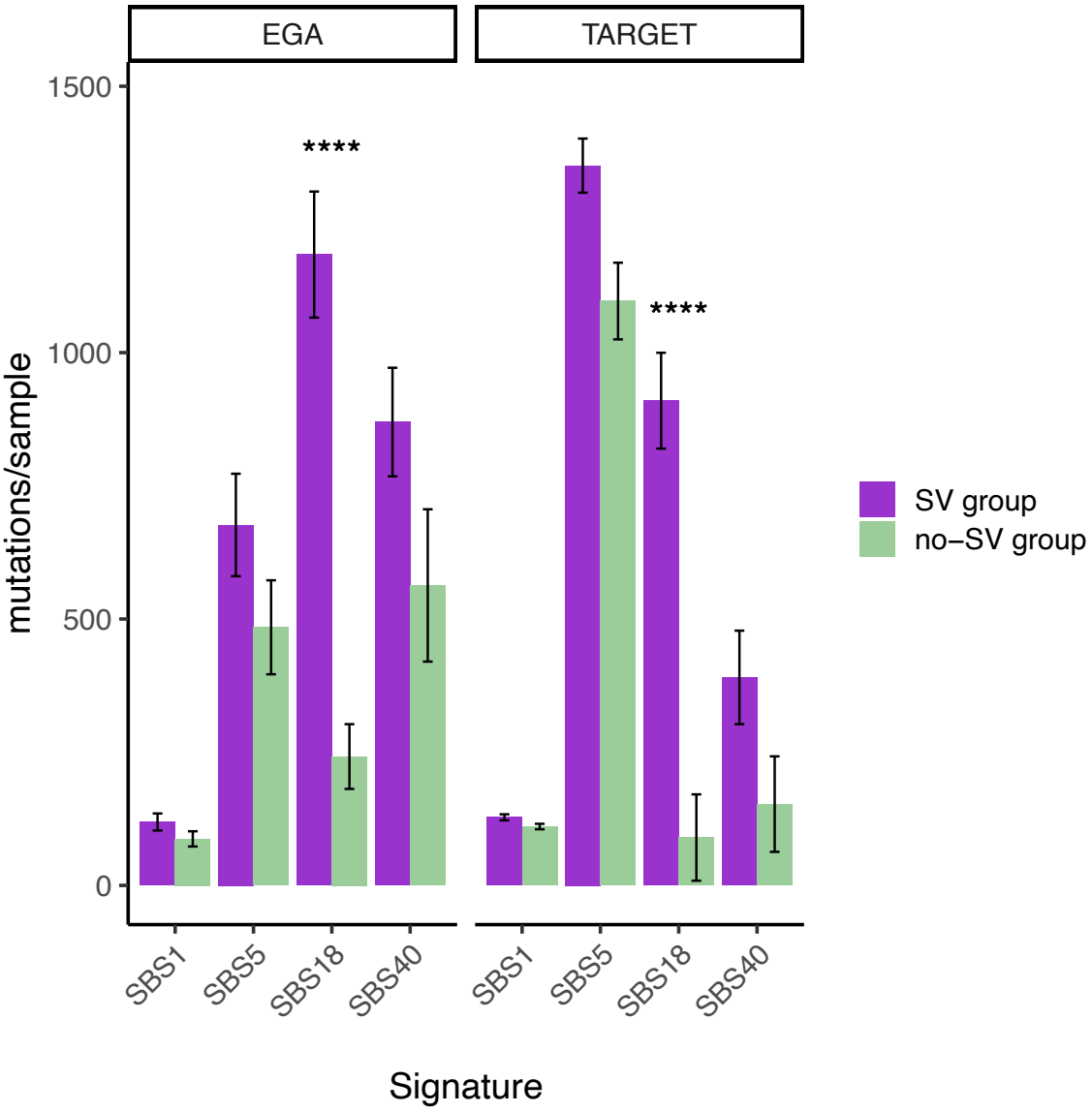

Figure 42. Absolute activity of SBS1, 5, 18 and 40 in SV and no-SV groups.

Bar plot showing the number of mutations per sample in SV and no-SV group in EGA and TARGET datasets. The error bars represent the standard errors. Significance was assessed through a univariate logistic regression. ****: $P < 10^{-4}$.

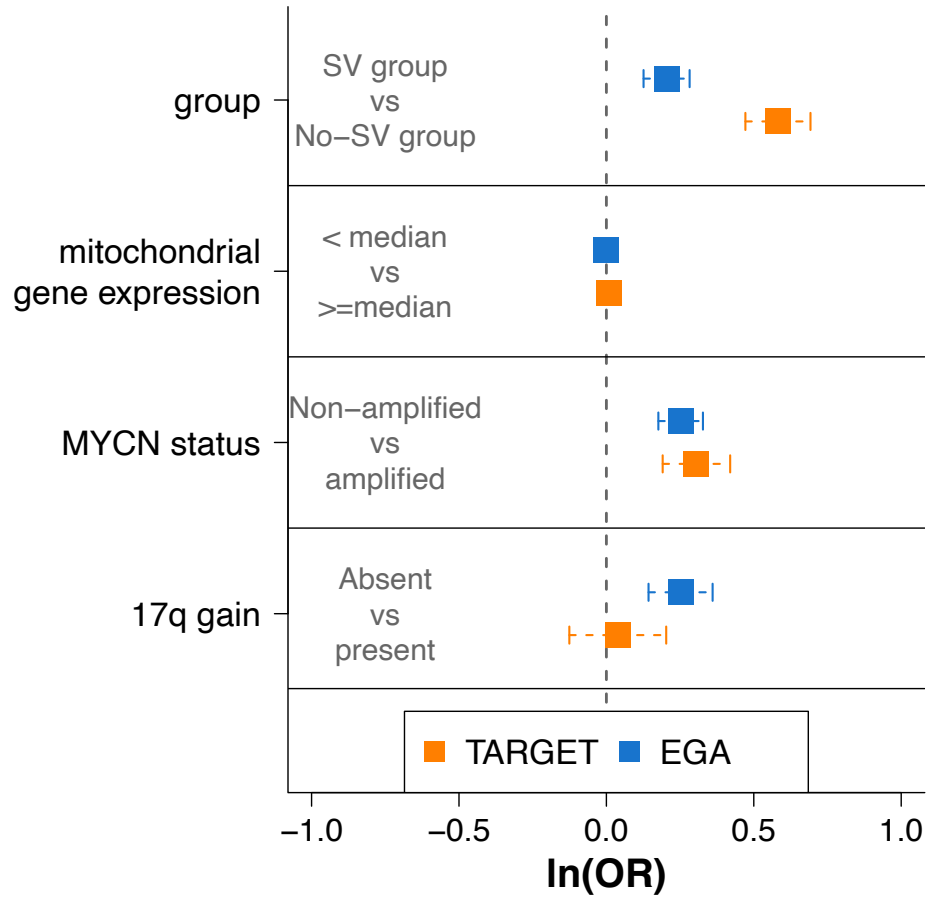

Figure 43. The enrichment of samples with SBS18 activity remained significative in a multivariate analysis using mitochondrial gene expression, MYCN status and 17q gain.

dot plot showing the results of a multivariate logistic regression comparing the presence of SBS18 activity and (from top to bottom) the SV group, mitochondrial gene expression, *MYCN* status and 17q gain. The squared dots and the dashed bars represent the estimate and the standard errors of the multivariate logistic regression, respectively.

4.3.3. SV group over-expressed DNA-repair related genes and under-expressed neuronal function and differentiation and synapse plasticity genes

Finally, we investigated gene-expression profile of the two groups of NBL samples (SV vs No-SV group). To this end, we leveraged paired-end RNA-seq data from a subset of TARGET (N=89) and EGA (N=140) samples. RNA-seq data from TARGET cohort were available as a publicly available matrix where the expression of each gene (rows) for each sample (columns) was expressed as FPKM. For samples in the EGA dataset, we processed BAM files as described by Hartlieb et al.[85] to obtain the raw read counts of each gene (rows) for each sample (columns), which were subsequently normalized to FPKM (see *Methods*). We performed a differential gene-expression analysis comparing the FPKM distribution of each gene of the SV and no-SV groups through a logistic regression, defining as differentially expressed (DE) genes that in both dataset that showed a p-value less than 0.01 and an absolute fold change of 1.5. Based on these criteria, a total of 170 and 145 protein-coding genes resulted over and under-expressed in the SV group, respectively. From an over ORA of biological processes resulted that pathways related to DNA-repair and control of cell cycle progression were over represented in the 170 SV group over-expressed genes (Figure 36). It is hypothesized that the over-expression of pathways related to DNA-repair and, more generally, to genome stability is a response to DNA damage in cancer[202]. Furthermore, in several tumors including melanoma[203], acute myeloid leukemia[204] and some breast cancer subtypes[205] the increased expression of DNA-repair is associated with poor outcome, suggesting the prognostic relevance of DNA-repair genes expression[205]. The 145 under-expressed genes in SV group mostly belonged to BPs of neurodevelopment, synapse plasticity and neuronal function (Figure 44). This result suggests that tumors from this subgroup are characterized by a lesser extent of differentiation compared to no-SV group tumors[206]. Importantly, the over and under-expression of the 170 and 145 genes in the SV group, respectively, was observed also when we considered only low to intermediate risk tumors (N=83, 29%), indicating the independence from the clinical status (Figure 45).

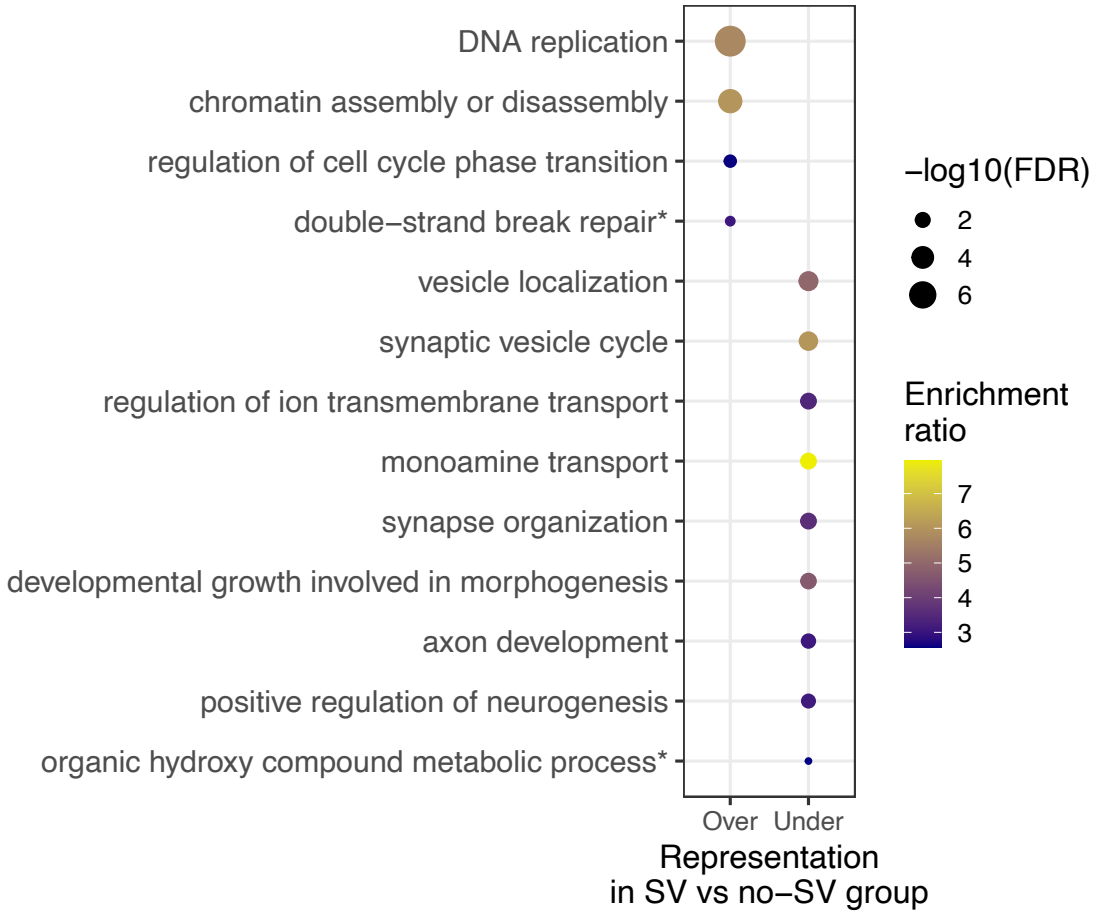

Figure 44. ORA results on SV group over and under-expressed genes.

Dot plot showing the enrichment ratio and the significance expressed as -$\log_{10}$(FDR) of an ORA performed on over (left) and under-expressed (right) genes in the SV group compared to the no-SV group. The BP enrichment was performed using the whole set of protein-coding genes as reference (see *Methods*). All the listed BPs were enriched with an FDR < 0.05, except the starred ones (FDR < 0.1). FDR: False Discovery Rate.

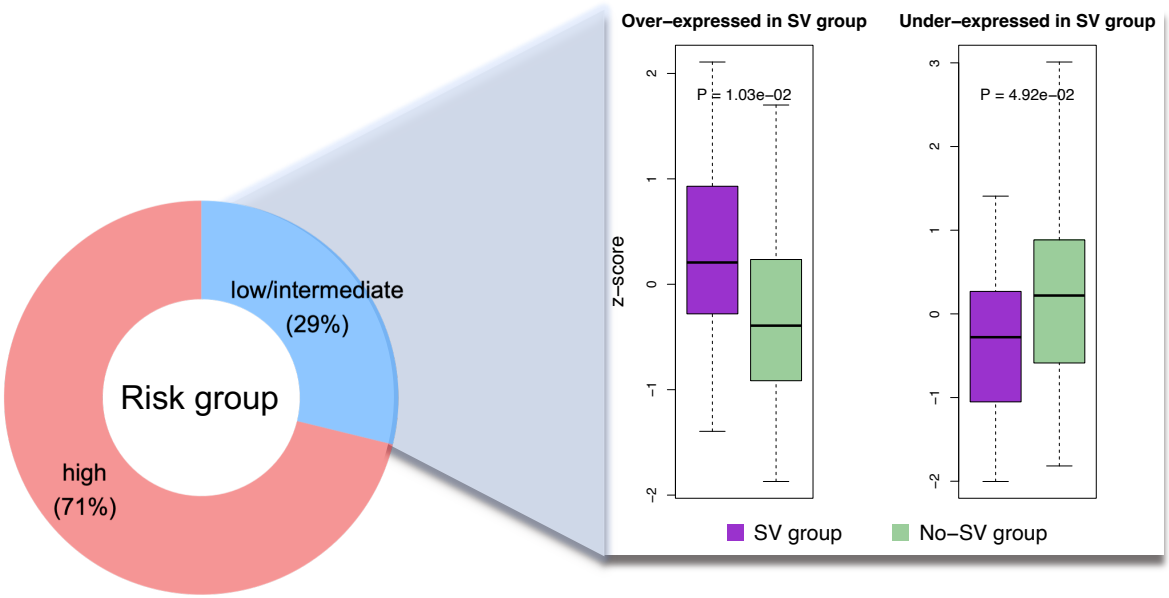

Figure 45. DEGs remained under and over represented in SV group when considering only the low to intermediate risk tumors.

Box plot showing the global expression of DEGs in the low-to-intermediate risk group expressed as z-score. The expression of the 170 SV group over-expressed genes resulted significantly increased in SV group when considering only low-to-intermediate risk samples (left bar plots). Similarly, the expression of the 145 SV group under-expressed genes resulted significantly decreased in SV group when considering only low-to-intermediate risk samples (right bar plots). P-values was computed through a two-sided Mann Whitney U-test.

4.4. Double-strand break repair genes were enriched in germline PVs in SV group

As discussed in the *Introduction*, the role of germline variation in cancer can go far beyond a simple predisposition, and often predisposes to the development of defined somatic events[108]. In order to determine a putative contribution of germline SNVs in NBL, in particular to the development of SVs, we investigated differences in terms of germline PVs between the SV and no-SV group. to this end, germline SNVs of TARGET samples were retrieved from publicly available VCF files, while those of EGA cohort were singularly called for each sample (see *Methods*). SNVs predicted to lead a functional consequence in exonic regions (also named coding SNVs) were classified as benign, likely benign, variant of unknown significance (VUS), likely pathogenic (LP) and pathogenic (P) based on the ACMG classification[207]. For our analysis, we selected only SNVs annotated as P or LP according to ACMG criteria. We obtained a total of 570 and 755 germline PVs in TARGET ($\mu = 4.194$) and EGA ($\mu = 4.191$) cohorts, respectively. In both datasets, the number of SNVs was comparable between SV and no-SV group (two-tailed Mann Whitney U-test $P > 0.1$) (Figure 46). To unbiasedly investigate differences in the germline background of the two groups, we first joined P/LP SNV of the two datasets and then performed two independent ORAs querying the WikiPathway cancer database[156] with the genes with at least a P/LP SNV in the *i*) SV group (N=557) and *ii)* in the no-SV group (N=108) using the whole set of protein-coding genes as reference. We observed an enrichment of the pathway WP4016 (DNA IR-damage and cellular response via ATR) in genes of the SV group at an FDR significance (Enrichment ratio = 3.46, FDR = 1.96×10^{-3}), but none in the no-SV group (Figure 47). WP4016 is a cancer-related pathway whose alterations have been previously associated to alteration in Double Strand Breaks (DSB) repair mechanisms[208–210]. 14 out of 80 genes of WP4016 pathway were affected by one or more PVs, involving a total of 36 samples (Table 6), and included notable pivotal TSGs for HR pathway (such as *CHEK2*, *BRCA1*/*2*, ATM and *BARD1* among the others) whose role in cancer predisposition is well established[211] (Figure 47). These results may indicate that germline P/LP SNVs affecting genes involved in DSB repair mechanisms, especially in the HR pathway, can predispose for the onset of NBL tumors with a defined SVs phenotype, characterized by a higher degree of genome instability, an abundance of SBS18 activity and a specific gene-expression pattern.

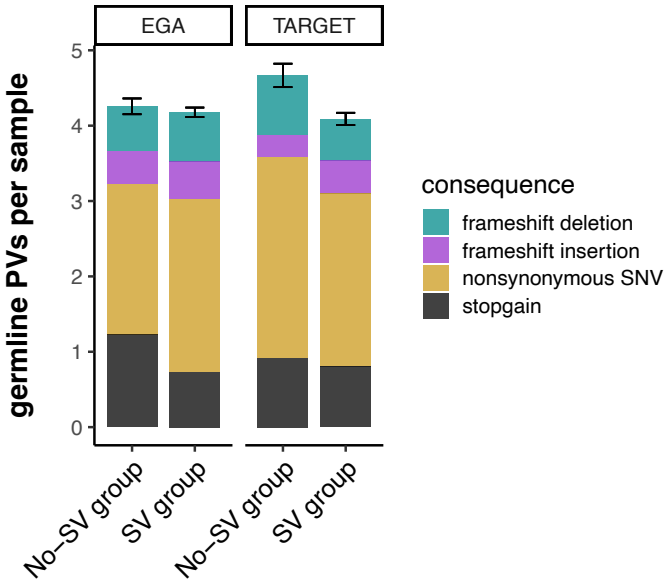

Figure 46. Mean number of germline PVs per SV group

Stacked bar plot showing the mean of germline PVs (according to ACMG criteria) in SV and no-SV group in EGA (left) and TARGET (right) datasets. Bars are colored based on exonic functional consequence of the SNV.

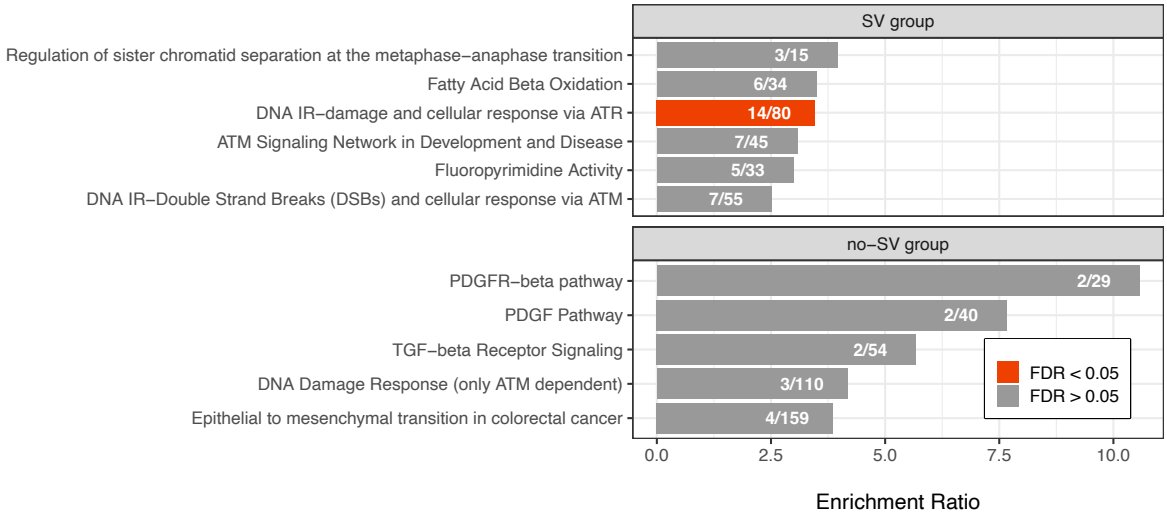

Figure 47. SV group was enriched in PVs in genes of DNA IR-damage and cellular response via ATR.

Bar plot showing the ORA in WikiPathway cancer database performed with genes with a germline PV in SV (top) and no-SV (bottom) groups. The numbers within the bars represent the fraction of genes with PVs on the total of genes of that pathway. The enrichment ratio on the x-axis is relative to the observed vs the expected gene overlap. In red is represented the WP4016 (DNA IR-damage and cellular response via ATR), which were the only enriched pathway.

variant ID	Gene	Functional consequence	ACMG Patogenicity criteria	samples
NM_000051.4:c.6067G>A	*ATM*	nonsynonymous SNV	PM1, PM2, PP3, PP5	4
NM_001271933.2:c.4213C>T	*CEP164*	stopgain	PVS1, PM2	2
NM_001024688.3:c.397C>T	*NBN*	nonsynonymous SNV	PM1, PM2, PP3, PP5	2
NM_000051.4:c.1229T>C	*ATM*	nonsynonymous SNV	PM1, PM2, PP3, PP5	2
NM_001113378.2:c.1573A>G	*FANCI*	nonsynonymous SNV	PM1, PM2, PP3, PP5	2
NM_007294.4:c.5177_5180del	*BRCA1*	frameshift deletion	PVS1, PS3, PM2, PP5	2
NM_000553.6:c.3785C>G	*WRN*	nonsynonymous SNV	PM1, PM2, PP3, PP5	2
NM_000059.4:c.2661_2662del	*BRCA2*	frameshift deletion	PVS1, PS3, PM2, PP5	1
NM_000059.4:c.3922G>T	*BRCA2*	stopgain	PVS1, PS3, PM2, PP5	1
NM_000059.4:c.8036A>G	*BRCA2*	nonsynonymous SNV	PM1, PM2, PP3, PP5	1
NM_000135.4:c.3391A>G	*FANCA*	nonsynonymous SNV	PS1, PM2, PP3, PP5	1
NM_203292.2:c.2377C>T	*RBBP8*	stopgain	PVS1, PM2	1
NM_000465.4:c.1921C>T	*BARD1*	stopgain	PVS1, PM2, PP5	1
NM_000465.4:c.448C>T	*BARD1*	stopgain	PVS1, PM2, PP3, PP5	1
NM_001127207.2:c.1271A>T	*SMARCAL1*	nonsynonymous SNV	PM1, PM2, PP3, PP5	1
NM_001005735.2:c.667C>T	*CHEK2*	nonsynonymous SNV	PM1, PM2, PP3, PP5	1
NM_001005735.2:c.562C>T	*CHEK2*	nonsynonymous SNV	PS1, PM1, PM2, PP3, PP5	1
NM_001172574.2:c.571del	*MCPH1*	frameshift deletion	PVS1, PM2	1
NM_000051.4:c.1010G>A	*ATM*	nonsynonymous SNV	PM1, PM2, PP3, PP5	1
NM_000051.4:c.7390T>C	*ATM*	nonsynonymous SNV	PM1, PM2, PP3, PP5	1
NM_000059.4:c.9155G>A	*BRCA2*	nonsynonymous SNV	PM1, PM2, PP3, PP5	1
NM_000059.4:c.10094_10095insGAATTATATC	*BRCA2*	frameshift insertion	PVS1, PM2	1
NM_024675.4:c.178C>T	*PALB2*	stopgain	PVS1, PM2, PP5	1
NM_007294.4:c.5266_5267insC	*BRCA1*	frameshift insertion	PVS1, PS3, PM2, PP5	1
NM_001005735.2:c.1031del	*CHEK2*	frameshift deletion	PVS1, PM2, PP5	1
NM_001005735.2:c.478A>G	*CHEK2*	nonsynonymous SNV	PM1, PM2, PP3, PP5	1
NM_001172574.2:c.182A>G	*MCPH1*	nonsynonymous SNV	PM1, PM2, PP3, PP5	1
NM_001322042.2:c.2166G>A	*MCPH1*	stopgain	PVS1, PM2, PP3	1
NM_000553.6:c.1436del	*WRN*	stopgain	PVS1, PM2	1
NM_000553.6:c.1717A>G	*WRN*	nonsynonymous SNV	PM1, PM2, PP3, PP5	1
NM_001024688.3:c.411_415del	*NBN*	frameshift deletion	PVS1, PM2, PP5	1
NM_001024688.3:c.37G>A	*NBN*	nonsynonymous SNV	PM1, PM2, PP3, PP5	1

Table 6. Germline PVs in genes of WP4016 pathway.

PVS1: LoF (stopgain or frameshift) causing a stop codon before 50bp the last exon, a splicing variant with a dbscSNV[212] score greater than 0.6;

PS1: nonsynonymous SNV causing the same aminoacidic change of a pathogenic variant in ClinVar database[143];

PS3: ClinVar pathogenic SNV whose level of evidence is either “practice guideline” or “reviewed by expert panel”;

PP5: ClinVar pathogenic SNV with limited evidence;

PP3: SNV predicted as probably pathogenic by various *in silico* prediction tools;

PM1: nonsynonymous SNV occurring in a domain with no known benign variants;

PM2: SNV in a recessive gene with a MAF < 0.5% or in a dominant gene with no public MAF available.

Finally, we observed that the observed distribution of PVs in WP4016 pathway across the various ethnicity of samples in the datasets (see Figure 12), and across the two dataset was comparable to the expected one (two-tailed Chi-squared P = 0.67 and P = 1, respectively), ruling out any bias due to population stratification or to a batch effect (Figure 48).

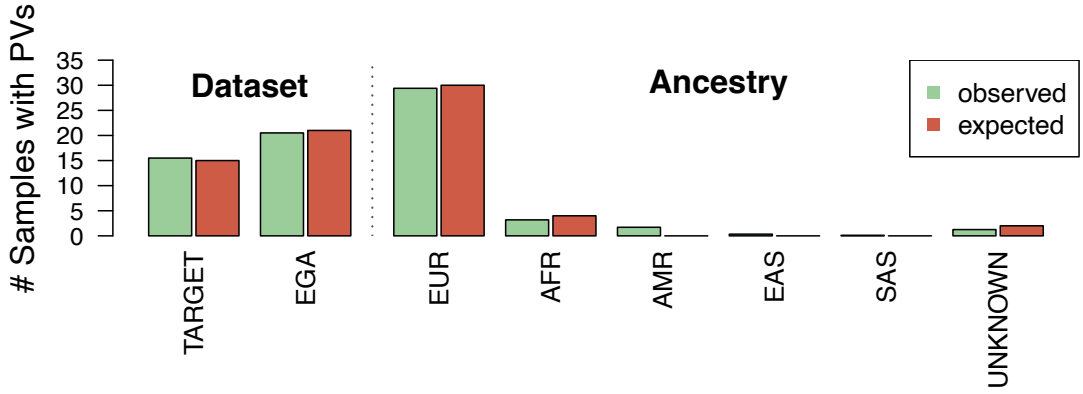

Figure 48. The expected and observed distribution of germline PVs in WP4016 genes was comparable across datasets and ethnicity.

Bar plot showing, on the y-axis, the number of observed (green) and expected (brown) PVs per dataset and per ancestry, which are specified on x-axis. AFR: African; AMR: Latino-American; EAS: East-Asian; EUR: Non-Finnish European; SAS: South-East-Asians

5. *Discussion*

One of the aims of this dissertation was to provide a comprehensive genomic profile of NBL. In detail, we downloaded, processed and analyzed WGS data of two independent NBL cohorts from two publicly queryable databases, TARGET (N=136) and EGA (N=180). Through the application and the integration of different bioinformatic tools and *in-house* pipelines, out of these samples we obtained germline and somatic SNVs, CNAs and genomic rearrangements, which were further processed for profiling purposes.

Concerning the somatic SNVs, we computed TMB and prioritized SNVs for the identification of putative cancer-driver genes. The TMB values were comparable between the two datasets and consistent with data from literature[36]. As expected, we found a solid association between TMB and markers of poor prognosis[166], with the solely exception of *MYCN* amplification, which is in line with recent evidence that suggests this driver alteration as occurring early during NBL development[213]. Nonetheless, only a trend – although negative – was observed between the TMB and the OS and EFS probability, both in univariate and in multivariate models.

Upon point mutations prioritization, *ALK* resulted the most frequently mutated gene, whose recurrent variants (F1174L, F1245V, R1275L and R1275Q among the others) were detected in both cohorts. We also detected key oncogenic NBL variants in genes like *KRAS*, *NRAS* and *FGFR1*. Furthermore, we identified 3 genes (*ESR1*, *MYH9* and *SKI*) whose mutations had not been previously reported. Two tumors carried missense variants in *ESR1* gene, one predicted as pathogenic by CADD, M-CAP and REVEL prediction tools and the other annotated as LP in ClinVar database. It is suggested that this gene is involved in the development of sympathetic nervous system and that its under-expression in NBL is associated to a worst prognosis[176]. *ESR1* has been shown to be an indirect target of *MYCN*. The latter promotes the transcription of some types of micro RNAs, in particular miR-18a and miR-19a, that repress the translation of *ESR1*, suggesting this gene as a probable TSG in NBL. Three samples had somatic predicted pathogenic missense SNVs in *MYH9*, which encodes a non-muscle protein that belongs to the myosin superfamily. Given its role in initiating tumor invasion and metastasis[214], *MYH9* was initially classified as an oncogene. However, while this applies for some solid cancers including gastric and esophageal cancer, in some others, such as skin and head and neck squamous carcinoma it acts as a TSG[215], a function that may be exercised through the stabilization of p53, although the precise mechanism is yet to be clarified[216]. in NBL, the exact identity of *MYH9* in NBL has not been established yet. Finally, *SKI* gene was affected by 3 SNVs, whose two non-sense and one missense predicted as pathogenic by all the three pathogenicity tools we used. As the previous two genes, also *SKI* can act as oncogene or as TGS. This duality reflects its

biological role in inhibiting the TGF-β pathway[174], which has been described to be both a tumor suppressor and an oncogenic pathway[217]. Although *SKI* function in NBL has not been yet elucidated, given the role of TGF-β signaling in promoting EMT in NBL[175] we suppose it to act as a TGS. Furthermore, *SKI* was the only one of these genes whose expression was lower in high-risk samples in both datasets, indicating a putative prognostic role of this gene, although additional studies are needed to confirm these findings. Finally, *SKI* maps at 1p36 locus which is frequently deleted in NB. This observation further suggests its tumor-suppressor role.

Point mutations in these genes occurred at a very low frequency (*MYH9* = 0.95%, *ESR1* = 0.63%, *SKI* = 0.95%), in line with other reported mutations in NBL. However, the alteration of these genes may not be limited to point mutations, but may also be involved in epigenetic changes. It is known that in NBL a series of TSGs may be inactivated by silencing mechanisms including DNA methylation, H3K9 methylation and H3K4 de-methylation, among the others[218]. Furthermore, with respect to *SKI* gene, it is well established that the EMT – which follows the activation of TGF-β pathway – is guided by a wave of transcriptional activations and repressions regulated by a series of epigenetic changes[219]. In this context, the reduced expression of *SKI* gene in high-risk tumors may be due to epigenetic mechanisms that need to be further elucidated.

Copy number analysis showed expected results in terms of types and frequency of typical and recurrent CNAs of NBL (*MYCN* amplification, 1p loss, 1q gain, 11q loss and 17q gain among the others), which were detected, in both cohorts, at similar frequency to that reported in previous studies[9,57,220]. As expected, we observed a positive correlation between segmental CNAs and poor-prognosis markers, and oppositely a positive correlation between numerical CNAs and good-prognosis markers. During the years, the contribution of segmental CNAs to the clinical outcome of NBL has become so solid that their detection has been incorporated in recent risk classification guidelines – the Children's Oncology Group (COG) risk classification system above all[221]. Our analysis detected 9 aneuploidies that were enriched in low to intermediate risk group (chr1 gain, chr2 gain, chr3 loss, chr4 loss, chr7 gain, chr11 loss, chr12 gain, chr17 gain and chr19 loss). We observed that the presence of at least one of these numerical CNA predicted survival in a multivariate model adjusting for known NBL poor-prognosis markers. Several studies highlight the positive effect on prognosis of numerical CNAs. Nevertheless, they take in consideration the co-presence of several chromosomal aneuploidies, or even to the whole chromosome asset[152,222,223], and only few studies focus on specific whole-chromosome CNAs[181,182,185]. Our analysis indicate that the presence of specific numerical CNAs predicts good prognosis in independent NBL cohorts, and in future may be implemented in clinical stratification criteria.

We finally assessed the presence and the role of genomic rearrangements in NBL – here referred to as SVs for simplicity – which to date remains poorly investigated in NBL. As expected, the number of SVs strongly correlated with poor-prognosis and with a diminished OS and OFS probability[19,88,224]. SV profiling identified known recurrent SVs (*TERT* rearrangements, t(1p-17q) and t(11q-17q)) and also other 5 unreported translocations (t(17q-19p), t(14q-17q), t(4p-17q), t(2p-3p) and t(1p-2p)) at a low frequency (< 5%). All these variants were associated to poor prognosis, and their breakpoints affected genes generally involved in synapse plasticity and neuronal development. The list of genes affected by these SVs, however, may be incomplete. In this dissertation, we did not investigate the alterations that such SVs may cause to the chromatin organization. It is indeed known that the presence of SVs in NBL may cause a re-arrangement in the transcriptional activity by disrupting the interaction between regulatory elements and close genes or by juxtaposing regulatory elements in proximity of otherwise distant genes, altering the global transcriptional network of the tumor[225]. To this end, further studies are needed to assess the impact that recurrent SVs may have on chromatin organization.

We observed that not all samples carried SVs. Therefore, we wanted to investigate phenotypical differences between samples which carried or not at least an SV, referred to as the SV and the no-SV group, respectively. SV group showed reduced OS and EFS probability in TARGET cohort, but only a trend in a multivariate model in the EGA dataset, although this result may be influenced by a strong co-linearity among clinical markers used as covariates[167]. Overall, SV group showed a higher degree of genetic instability, with the exclusion of numerical CNAs with which was observed no or a negative correlation. From mutational signature analysis we report an increase of SBS18 activity in SV group, even when adjusting for other factors which have been shown to correlate with this SBS (17q gain, *MYCN* amplification and mitochondrial gene expression)[152].

The signature SBS18 is highly characteristic of neuroblastoma (NBL). Studies have shown that samples with this signature predominantly exhibit C>A transversions. This mutation pattern is largely attributed to the oxidation of guanine bases into 8-oxoG as a result of ROS production[226,227]. Furthermore, DNA damage, particularly DSB, is known to induce ROS in a consistent and generalized stress response throughout the cell[228].

Our findings suggest that SVs, which occur following DSBs, may contribute to the generation of ROS. This, in turn, leads to C>A mutations and the emergence of the SBS18 signature. Interestingly, the TMB is notably higher in the SV group, which is primarily due to mutations linked to SBS18. This observation implies that the presence of SVs and the associated genetic instability could elevate the frequency of SBS18 mutations. These mutations encompass the majority of recurrent driver mutations in NBL[152].

We also observed differences in gene expression between the two groups. Firstly, from DE analysis resulted that SV group over-expressed DNA-repair and cell cycle checkpoint genes. This unexpected result may reflect a compensatory increase and reliance in DNA-repair genes in tumors with an increased degree of genetic instability to guarantee a minimum control on DNA-damage and of cell cycle progression[229]. In this context, patients with this expression pattern may benefit for specific therapies targeting DNA-repair genes in a mechanism of synthetic lethality[230]. On the other hand, in line with evidence reported by Lopez and colleagues[88], SV group downregulated genes involved in neurogenesis, neuronal development and synapse formation and organization, suggesting a lesser extent of differentiation in these tumors[231]. In our quest to understand the potential genetic predisposition contributing to the SV group phenotype in NBL patients, we explored the role of germline DNA. Our approach involved selecting coding and rare germline variants classified as P/LP based on ACMG criteria. We then identified genes harboring these variants. To assess the involvement of these genes in cancer-related pathways, we conducted two independent over-representation analyses in the SV and in no-SV group using the WikiPathway cancer database, which contains a comprehensive catalog of cancer-related pathways[156].

Our analysis revealed a significant enrichment of genes involved in the DNA damage response to ionizing radiation and cellular response via the ATR pathway (WP4016) within the SV group. Notably, 14 out of 80 genes in this pathway were mutated in at least one sample from the SV group. This includes several TSGs integral to DSB repair, with germline variants etiologically linked to various cancer predisposition syndromes. For example, pathogenic variants in *BRCA1* and *BRCA2* are associated with breast and ovarian cancer susceptibility, with *BRCA1* recently identified by our team as a predisposition gene for NBL[86]. Similarly, germline pathogenic variants in *CHEK2* and *ATM*, crucial for initiating DSB repair signaling, have been implicated in predisposition to a spectrum of cancers, including lymphomas, leukemias, thyroid carcinoma, melanoma, and colon cancer[232,233]. Moreover, germline variations in *BARD1*, identified in 2 patients with P/LP SNVs, are linked to DNA repair defects and consequently to genetic instability in NBL[35].

The underlying mechanism for tumorigenesis in these cases appears to be an innate deficiency in DNA repair processes, particularly HR, leading to a reduced capacity to repair DNA damage and maintain genomic integrity[234]. Our analysis of the correlation between germline and somatic genetic changes suggests that germline variations in DNA repair genes, which predispose to cancer, may promote increased somatic genetic instability, ultimately contributing to malignant transformation. While additional computational and experimental studies are necessary to further validate and elaborate on our findings, the data

we have gathered offers valuable insight into the mechanisms by which cancer-predisposing germline variants could initiate NBL.

6. Conclusions

Our exhaustive whole-genome sequencing analysis has revealed a spectrum of novel genomic alterations that are distinctive to NBL tumors. We have identified rare point mutations in the *SKI*, *ESR1* and *MYH9* genes, which may act as oncogenic drivers, marking a significant step forward in our understanding of NBL pathogenesis. These mutations could serve as novel targets for therapeutic intervention, potentially leading to the development of precision medicine strategies tailored to individual genetic profiles.

Furthermore, our research has uncovered novel SVs that occur at a low frequency but affect genes that are promising candidates for cancer research. These findings may pave the way for the discovery of new biomarkers for early detection and prognosis of NBL.

The association we found between specific aneuploidies and the clinical outcomes of NBL patients is particularly noteworthy. This correlation could be instrumental in refining risk stratification models, leading to more personalized treatment plans and potentially improving survival rates. Our data suggest that incorporating genetic screening for these aneuploidies could significantly enhance the predictive accuracy of current risk assessment protocols.

Finally, our report highlights the enrichment of P/LP germline variants in DNA repair genes among patients with genetically unstable tumors. This underscores the possible contribution of inherited genetic factors to tumor behavior and aggressiveness in pediatric NBL.

In conclusion, these genetic insights provide a foundation for future clinical applications, including the development of targeted therapies and enhancement of diagnostic precision. The potential to significantly improve patient outcomes by integrating these genetic markers into clinical practice represents a transformative advance in the fight against this challenging pediatric malignancy.

7. References

1. Howman-Giles, R., Shaw, P. J., Uren, R. F. & Chung, D. K. V. Neuroblastoma and other neuroendocrine tumors. *Semin. Nucl. Med.* **37**, 286–302 (2007).
2. Okawa, S. & Saika, K. International variations in neuroblastoma incidence in children and adolescents. *Jpn. J. Clin. Oncol.* **52**, 656–658 (2022).
3. Luksch, R. *et al.* Neuroblastoma (Peripheral neuroblastic tumours). *Crit. Rev. Oncol. Hematol.* **107**, 163–181 (2016).
4. Delloye-Bourgeois, C. & Castellani, V. Hijacking of Embryonic Programs by Neural Crest-Derived Neuroblastoma: From Physiological Migration to Metastatic Dissemination. *Front. Mol. Neurosci.* **12**, 52 (2019).
5. Anderson, D. J., Carnahan, J. F., Michelsohn, A. & Patterson, P. H. Antibody markers identify a common progenitor to sympathetic neurons and chromaffin cells in vivo and reveal the timing of commitment to neuronal differentiation in the sympathoadrenal lineage. *J. Neurosci. Off. J. Soc. Neurosci.* **11**, 3507–3519 (1991).
6. Matthay, K. K. *et al.* Neuroblastoma. *Nat. Rev. Dis. Primer* **2**, 16078 (2016).
7. Marshall, G. M. *et al.* The prenatal origins of cancer. *Nat. Rev. Cancer* **14**, 277–289 (2014).
8. Gomez, R. L., Ibragimova, S., Ramachandran, R., Philpott, A. & Ali, F. R. Tumoral heterogeneity in neuroblastoma. *Biochim. Biophys. Acta Rev. Cancer* **1877**, 188805 (2022).
9. Pugh, T. J. *et al.* The genetic landscape of high-risk neuroblastoma. *Nat. Genet.* **45**, 279–284 (2013).
10. Grimes, T., Walker, A. R., Datta, S. & Datta, S. Predicting survival times for neuroblastoma patients using RNA-seq expression profiles. *Biol. Direct* **13**, 11 (2018).
11. Brady, S. W. *et al.* Pan-neuroblastoma analysis reveals age- and signature-associated driver alterations. *Nat. Commun.* **11**, 5183 (2020).
12. Lundberg, K. I., Treis, D. & Johnsen, J. I. Neuroblastoma Heterogeneity, Plasticity, and Emerging Therapies. *Curr. Oncol. Rep.* **24**, 1053–1062 (2022).
13. Pinto, N. R. *et al.* Advances in Risk Classification and Treatment Strategies for Neuroblastoma. *J. Clin. Oncol. Off. J. Am. Soc. Clin. Oncol.* **33**, 3008–3017 (2015).
14. Cohn, S. L. *et al.* The International Neuroblastoma Risk Group (INRG) classification system: an INRG Task Force report. *J. Clin. Oncol. Off. J. Am. Soc. Clin. Oncol.* **27**, 289–297 (2009).
15. Brodeur, G. M. Neuroblastoma: clinical significance of genetic abnormalities. *Cancer Surv.* **9**, 673–688 (1990).
16. Brodeur, G. M. *et al.* Revisions of the international criteria for neuroblastoma diagnosis, staging, and response to treatment. *J. Clin. Oncol. Off. J. Am. Soc. Clin. Oncol.* **11**, 1466–1477 (1993).
17. Sokol, E. & Desai, A. V. The Evolution of Risk Classification for Neuroblastoma. *Child. Basel Switz.* **6**, 27 (2019).
18. Raabe, E. H. *et al.* Prevalence and functional consequence of PHOX2B mutations in neuroblastoma. *Oncogene* **27**, 469–476 (2008).
19. Tonini, G. P. & Capasso, M. Genetic predisposition and chromosome instability in neuroblastoma. *Cancer Metastasis Rev.* **39**, 275–285 (2020).
20. Heck, J. E., Ritz, B., Hung, R. J., Hashibe, M. & Boffetta, P. The epidemiology of neuroblastoma: a review. *Paediatr. Perinat. Epidemiol.* **23**, 125–143 (2009).
21. De Roos, A. J. *et al.* Parental occupational exposures to electromagnetic fields and radiation and the incidence of neuroblastoma in offspring. *Epidemiol. Camb. Mass* **12**, 508–517 (2001).
22. Michalek, A. M. *et al.* Gravid health status, medication use, and risk of neuroblastoma. *Am. J. Epidemiol.* **143**, 996–1001 (1996).
23. Cook, M. N. *et al.* Maternal medication use and neuroblastoma in offspring. *Am. J. Epidemiol.* **159**, 721–731 (2004).

24. French, A. E. *et al.* Folic acid food fortification is associated with a decline in neuroblastoma. *Clin. Pharmacol. Ther.* **74**, 288–294 (2003).
25. Pattyn, A., Morin, X., Cremer, H., Goridis, C. & Brunet, J. F. The homeobox gene Phox2b is essential for the development of autonomic neural crest derivatives. *Nature* **399**, 366–370 (1999).
26. Rohrer, T., Trachsel, D., Engelcke, G. & Hammer, J. Congenital central hypoventilation syndrome associated with Hirschsprung's disease and neuroblastoma: case of multiple neurocristopathies. *Pediatr. Pulmonol.* **33**, 71–76 (2002).
27. Wulf, A. M., Moreno, M. M., Paka, C., Rampasekova, A. & Liu, K. J. Defining Pathological Activities of ALK in Neuroblastoma, a Neural Crest-Derived Cancer. *Int. J. Mol. Sci.* **22**, 11718 (2021).
28. Mossé, Y. P. *et al.* Identification of ALK as a major familial neuroblastoma predisposition gene. *Nature* **455**, 930–935 (2008).
29. de Pontual, L. *et al.* Germline gain-of-function mutations of ALK disrupt central nervous system development. *Hum. Mutat.* **32**, 272–276 (2011).
30. Bresler, S. C. *et al.* ALK mutations confer differential oncogenic activation and sensitivity to ALK inhibition therapy in neuroblastoma. *Cancer Cell* **26**, 682–694 (2014).
31. van Limpt, V. *et al.* The Phox2B homeobox gene is mutated in sporadic neuroblastomas. *Oncogene* **23**, 9280–9288 (2004).
32. Serra, A. *et al.* Rare occurrence of PHOX2b mutations in sporadic neuroblastomas. *J. Pediatr. Hematol. Oncol.* **30**, 728–732 (2008).
33. Cimmino, F., Formicola, D. & Capasso, M. Dualistic Role of BARD1 in Cancer. *Genes* **8**, 375 (2017).
34. Capasso, M. *et al.* Common variations in BARD1 influence susceptibility to high-risk neuroblastoma. *Nat. Genet.* **41**, 718–723 (2009).
35. Randall, M. P. *et al.* BARD1 germline variants induce haploinsufficiency and DNA repair defects in neuroblastoma. *J. Natl. Cancer Inst.* djad182 (2023) doi:10.1093/jnci/djad182.
36. Gröbner, S. N. *et al.* The landscape of genomic alterations across childhood cancers. *Nature* **555**, 321–327 (2018).
37. Capasso, M. & Diskin, S. J. Genetics and genomics of neuroblastoma. *Cancer Treat. Res.* **155**, 65–84 (2010).
38. Maris, J. M. Recent advances in neuroblastoma. *N. Engl. J. Med.* **362**, 2202–2211 (2010).
39. Pandita, A. *et al.* Relational mapping of MYCN and DDXI in band 2p24 and analysis of amplicon arrays in double minute chromosomes and homogeneously staining regions by use of free chromatin FISH. *Genes. Chromosomes Cancer* **20**, 243–252 (1997).
40. Li, H.-L. *et al.* A Review of the Regulatory Mechanisms of N-Myc on Cell Cycle. *Mol. Basel Switz.* **28**, 1141 (2023).
41. Boeva, V. *et al.* Heterogeneity of neuroblastoma cell identity defined by transcriptional circuitries. *Nat. Genet.* **49**, 1408–1413 (2017).
42. Durbin, A. D. *et al.* Selective gene dependencies in MYCN-amplified neuroblastoma include the core transcriptional regulatory circuitry. *Nat. Genet.* **50**, 1240–1246 (2018).
43. Wu, K. J. *et al.* Direct activation of TERT transcription by c-MYC. *Nat. Genet.* **21**, 220–224 (1999).
44. Counter, C. M. *et al.* Telomerase activity is restored in human cells by ectopic expression of hTERT (hEST2), the catalytic subunit of telomerase. *Oncogene* **16**, 1217–1222 (1998).
45. Peifer, M. *et al.* Telomerase activation by genomic rearrangements in high-risk neuroblastoma. *Nature* **526**, 700–704 (2015).
46. Valentijn, L. J. *et al.* TERT rearrangements are frequent in neuroblastoma and identify aggressive tumors. *Nat. Genet.* **47**, 1411–1414 (2015).

47. Rosswog, C. *et al.* Genomic ALK alterations in primary and relapsed neuroblastoma. *Br. J. Cancer* **128**, 1559–1571 (2023).
48. Aubry, A. *et al.* Peptides derived from the dependence receptor ALK are proapoptotic for ALK-positive tumors. *Cell Death Dis.* **6**, e1736 (2015).
49. Mossé, Y. P. *et al.* Safety and activity of crizotinib for paediatric patients with refractory solid tumours or anaplastic large-cell lymphoma: a Children's Oncology Group phase 1 consortium study. *Lancet Oncol.* **14**, 472–480 (2013).
50. Udugama, M. *et al.* Histone variant H3.3 provides the heterochromatic H3 lysine 9 tri-methylation mark at telomeres. *Nucleic Acids Res.* **43**, 10227–10237 (2015).
51. van Gerven, M. R. *et al.* Mutational spectrum of ATRX aberrations in neuroblastoma and associated patient and tumor characteristics. *Cancer Sci.* **113**, 2167–2178 (2022).
52. Eleveld, T. F. *et al.* Relapsed neuroblastomas show frequent RAS-MAPK pathway mutations. *Nat. Genet.* **47**, 864–871 (2015).
53. Mertens, F., Mandahl, N., Mitelman, F. & Heim, S. Cytogenetic analysis in the examination of solid tumors in children. *Pediatr. Hematol. Oncol.* **11**, 361–377 (1994).
54. Gilbert, F., Balaban, G., Moorhead, P., Bianchi, D. & Schlesinger, H. Abnormalities of chromosome 1p in human neuroblastoma tumors and cell lines. *Cancer Genet. Cytogenet.* **7**, 33–42 (1982).
55. Breen, C. J., O'Meara, A., McDermott, M., Mullarkey, M. & Stallings, R. L. Coordinate deletion of chromosome 3p and 11q in neuroblastoma detected by comparative genomic hybridization. *Cancer Genet. Cytogenet.* **120**, 44–49 (2000).
56. Tong, C. Y. *et al.* Central neurocytomas are genetically distinct from oligodendrogliomas and neuroblastomas. *Histopathology* **37**, 160–165 (2000).
57. Depuydt, P. *et al.* Genomic Amplifications and Distal 6q Loss: Novel Markers for Poor Survival in High-risk Neuroblastoma Patients. *J. Natl. Cancer Inst.* **110**, 1084–1093 (2018).
58. Chen, J. & Coppola, G. Bioinformatics and genomic databases. *Handb. Clin. Neurol.* **147**, 75–92 (2018).
59. Ehret, G. B. Genome-wide association studies: contribution of genomics to understanding blood pressure and essential hypertension. *Curr. Hypertens. Rep.* **12**, 17–25 (2010).
60. Cai, L. *et al.* Genome-wide association analysis of type 2 diabetes in the EPIC-InterAct study. *Sci. Data* **7**, 393 (2020).
61. Sato, G. *et al.* Pan-cancer and cross-population genome-wide association studies dissect shared genetic backgrounds underlying carcinogenesis. *Nat. Commun.* **14**, 3671 (2023).
62. Hong, H., Xu, L. & Tong, W. Assessing consistency between versions of genotype-calling algorithm Birdseed for the Genome-Wide Human SNP Array 6.0 using HapMap samples. *Adv. Exp. Med. Biol.* **680**, 355–360 (2010).
63. Dehghan, A. Genome-Wide Association Studies. *Methods Mol. Biol. Clifton NJ* **1793**, 37–49 (2018).
64. Maris, J. M. *et al.* Chromosome 6p22 locus associated with clinically aggressive neuroblastoma. *N. Engl. J. Med.* **358**, 2585–2593 (2008).
65. Wang, K. *et al.* Integrative genomics identifies LMO1 as a neuroblastoma oncogene. *Nature* **469**, 216–220 (2011).
66. Zhu, S. *et al.* LMO1 Synergizes with MYCN to Promote Neuroblastoma Initiation and Metastasis. *Cancer Cell* **32**, 310-323.e5 (2017).
67. Diskin, S. J. *et al.* Common variation at 6q16 within HACE1 and LIN28B influences susceptibility to neuroblastoma. *Nat. Genet.* **44**, 1126–1130 (2012).
68. Capasso, M. *et al.* Replication of GWAS-identified neuroblastoma risk loci strengthens the role of BARD1 and affirms the cumulative effect of genetic variations on disease susceptibility. *Carcinogenesis* **34**, 605–611 (2013).

69. He, J. *et al.* Genetic Variations of GWAS-Identified Genes and Neuroblastoma Susceptibility: a Replication Study in Southern Chinese Children. *Transl. Oncol.* **10**, 936–941 (2017).
70. Tam, V. *et al.* Benefits and limitations of genome-wide association studies. *Nat. Rev. Genet.* **20**, 467–484 (2019).
71. Mardis, E. R. Next-generation sequencing platforms. *Annu. Rev. Anal. Chem. Palo Alto Calif* **6**, 287–303 (2013).
72. Pereira, R., Oliveira, J. & Sousa, M. Bioinformatics and Computational Tools for Next-Generation Sequencing Analysis in Clinical Genetics. *J. Clin. Med.* **9**, 132 (2020).
73. Ji, F. & Sadreyev, R. I. RNA-seq: Basic Bioinformatics Analysis. *Curr. Protoc. Mol. Biol.* **124**, e68 (2018).
74. Servant, N. Bioinformatics Methods for ChIP-seq Histone Analysis. *Methods Mol. Biol. Clifton NJ* **2529**, 267–293 (2022).
75. Ng, S. B. *et al.* Targeted capture and massively parallel sequencing of 12 human exomes. *Nature* **461**, 272–276 (2009).
76. Rotunno, M. *et al.* A Systematic Literature Review of Whole Exome and Genome Sequencing Population Studies of Genetic Susceptibility to Cancer. *Cancer Epidemiol. Biomark. Prev. Publ. Am. Assoc. Cancer Res. Cosponsored Am. Soc. Prev. Oncol.* **29**, 1519–1534 (2020).
77. Xiao, W. *et al.* Toward best practice in cancer mutation detection with whole-genome and whole-exome sequencing. *Nat. Biotechnol.* **39**, 1141–1150 (2021).
78. Ng, P. C. & Kirkness, E. F. Whole genome sequencing. *Methods Mol. Biol. Clifton NJ* **628**, 215–226 (2010).
79. Ellingford, J. M. *et al.* Recommendations for clinical interpretation of variants found in non-coding regions of the genome. *Genome Med.* **14**, 73 (2022).
80. Kosugi, S. *et al.* Comprehensive evaluation of structural variation detection algorithms for whole genome sequencing. *Genome Biol.* **20**, 117 (2019).
81. Chu, Y. & Corey, D. R. RNA sequencing: platform selection, experimental design, and data interpretation. *Nucleic Acid Ther.* **22**, 271–274 (2012).
82. Kolodziejczyk, A. A., Kim, J. K., Svensson, V., Marioni, J. C. & Teichmann, S. A. The technology and biology of single-cell RNA sequencing. *Mol. Cell* **58**, 610–620 (2015).
83. Janoueix-Lerosey, I. *et al.* Somatic and germline activating mutations of the ALK kinase receptor in neuroblastoma. *Nature* **455**, 967–970 (2008).
84. Ackermann, S. *et al.* A mechanistic classification of clinical phenotypes in neuroblastoma. *Science* **362**, 1165–1170 (2018).
85. Hartlieb, S. A. *et al.* Alternative lengthening of telomeres in childhood neuroblastoma from genome to proteome. *Nat. Commun.* **12**, 1269 (2021).
86. Bonfiglio, F. *et al.* Inherited rare variants in homologous recombination and neurodevelopmental genes are associated with increased risk of neuroblastoma. *EBioMedicine* **87**, 104395 (2023).
87. Mahmoud, M. *et al.* Structural variant calling: the long and the short of it. *Genome Biol.* **20**, 246 (2019).
88. Lopez, G. *et al.* Somatic structural variation targets neurodevelopmental genes and identifies SHANK2 as a tumor suppressor in neuroblastoma. *Genome Res.* **30**, 1228–1242 (2020).
89. Stark, B. *et al.* der(11)t(11;17): a distinct cytogenetic pathway of advanced stage neuroblastoma (NBL) - detected by spectral karyotyping (SKY). *Cancer Lett.* **197**, 75–79 (2003).
90. Tate, J. G. *et al.* COSMIC: the Catalogue Of Somatic Mutations In Cancer. *Nucleic Acids Res.* **47**, D941–D947 (2019).
91. Alexandrov, L. B. *et al.* Signatures of mutational processes in human cancer. *Nature* **500**, 415–421 (2013).
92. Thatikonda, V. *et al.* Comprehensive analysis of mutational signatures reveals

distinct patterns and molecular processes across 27 pediatric cancers. *Nat. Cancer* **4**, 276–289 (2023).
93. Rodriguez-Fos, E. *et al.* Mutational topography reflects clinical neuroblastoma heterogeneity. *Cell Genomics* **3**, 100402 (2023).
94. Nik-Zainal, S. *et al.* Mutational processes molding the genomes of 21 breast cancers. *Cell* **149**, 979–993 (2012).
95. Bruskov, V. I., Malakhova, L. V., Masalimov, Z. K. & Chernikov, A. V. Heat-induced formation of reactive oxygen species and 8-oxoguanine, a biomarker of damage to DNA. *Nucleic Acids Res.* **30**, 1354–1363 (2002).
96. van Groningen, T. *et al.* Neuroblastoma is composed of two super-enhancer-associated differentiation states. *Nat. Genet.* **49**, 1261–1266 (2017).
97. Westerhout, E. M. *et al.* Mesenchymal-Type Neuroblastoma Cells Escape ALK Inhibitors. *Cancer Res.* **82**, 484–496 (2022).
98. Koboldt, D. C. Best practices for variant calling in clinical sequencing. *Genome Med.* **12**, 91 (2020).
99. Knudson, A. G. Mutation and cancer: statistical study of retinoblastoma. *Proc. Natl. Acad. Sci. U. S. A.* **68**, 820–823 (1971).
100. Nichols, C. A. *et al.* Loss of heterozygosity of essential genes represents a widespread class of potential cancer vulnerabilities. *Nat. Commun.* **11**, 2517 (2020).
101. Takita, J., Hayashi, Y. & Yokota, J. Loss of heterozygosity in neuroblastomas--an overview. *Eur. J. Cancer Oxf. Engl. 1990* **33**, 1971–1973 (1997).
102. Tuupanen, S. *et al.* Allelic imbalance at rs6983267 suggests selection of the risk allele in somatic colorectal tumor evolution. *Cancer Res.* **68**, 14–17 (2008).
103. Sugimachi, K. *et al.* Allelic imbalance at an 8q24 oncogenic SNP is involved in activating MYC in human colorectal cancer. *Ann. Surg. Oncol.* **21 Suppl 4**, S515-521 (2014).
104. Hienonen, T. *et al.* Preferential amplification of AURKA 91A (Ile31) in familial colorectal cancers. *Int. J. Cancer* **118**, 505–508 (2006).
105. LaFramboise, T., Dewal, N., Wilkins, K., Pe'er, I. & Freedman, M. L. Allelic selection of amplicons in glioblastoma revealed by combining somatic and germline analysis. *PLoS Genet.* **6**, e1001086 (2010).
106. Dworkin, A. M. *et al.* Germline variation controls the architecture of somatic alterations in tumors. *PLoS Genet.* **6**, e1001136 (2010).
107. Olcaydu, D. *et al.* A common JAK2 haplotype confers susceptibility to myeloproliferative neoplasms. *Nat. Genet.* **41**, 450–454 (2009).
108. Ramroop, J. R., Gerber, M. M. & Toland, A. E. Germline Variants Impact Somatic Events during Tumorigenesis. *Trends Genet. TIG* **35**, 515–526 (2019).
109. Lu, Y. *et al.* Most common 'sporadic' cancers have a significant germline genetic component. *Hum. Mol. Genet.* **23**, 6112–6118 (2014).
110. Carter, H. *et al.* Interaction Landscape of Inherited Polymorphisms with Somatic Events in Cancer. *Cancer Discov.* **7**, 410–423 (2017).
111. Chu, E. C. & Tarnawski, A. S. PTEN regulatory functions in tumor suppression and cell biology. *Med. Sci. Monit. Int. Med. J. Exp. Clin. Res.* **10**, RA235-241 (2004).
112. Shoushtari, A. N. & Carvajal, R. D. GNAQ and GNA11 mutations in uveal melanoma. *Melanoma Res.* **24**, 525–534 (2014).
113. Spurdle, A. B. *et al.* Refined histopathological predictors of BRCA1 and BRCA2 mutation status: a large-scale analysis of breast cancer characteristics from the BCAC, CIMBA, and ENIGMA consortia. *Breast Cancer Res. BCR* **16**, 3419 (2014).
114. Mulligan, A. M. *et al.* Common breast cancer susceptibility alleles are associated with tumour subtypes in BRCA1 and BRCA2 mutation carriers: results from the Consortium of Investigators of Modifiers of BRCA1/2. *Breast Cancer Res. BCR* **13**, R110 (2011).
115. Stevens, K. N. *et al.* Common breast cancer susceptibility loci are associated with

triple-negative breast cancer. *Cancer Res.* **71**, 6240–6249 (2011).
116. Stevens, K. N., Vachon, C. M. & Couch, F. J. Genetic susceptibility to triple-negative breast cancer. *Cancer Res.* **73**, 2025–2030 (2013).
117. Buisson, R. *et al.* Cooperation of breast cancer proteins PALB2 and piccolo BRCA2 in stimulating homologous recombination. *Nat. Struct. Mol. Biol.* **17**, 1247–1254 (2010).
118. Waszak, S. M. *et al.* Spectrum and prevalence of genetic predisposition in medulloblastoma: a retrospective genetic study and prospective validation in a clinical trial cohort. *Lancet Oncol.* **19**, 785–798 (2018).
119. Singh, V. K., Rastogi, A., Hu, X., Wang, Y. & De, S. Mutational signature SBS8 predominantly arises due to late replication errors in cancer. *Commun. Biol.* **3**, 421 (2020).
120. Rausch, T. *et al.* Genome sequencing of pediatric medulloblastoma links catastrophic DNA rearrangements with TP53 mutations. *Cell* **148**, 59–71 (2012).
121. Palles, C. *et al.* Germline MBD4 deficiency causes a multi-tumor predisposition syndrome. *Am. J. Hum. Genet.* **109**, 953–960 (2022).
122. Marty, R. *et al.* MHC-I Genotype Restricts the Oncogenic Mutational Landscape. *Cell* **171**, 1272-1283.e15 (2017).
123. Lappalainen, I. *et al.* DbVar and DGVa: public archives for genomic structural variation. *Nucleic Acids Res.* **41**, D936-941 (2013).
124. Sudmant, P. H. *et al.* An integrated map of structural variation in 2,504 human genomes. *Nature* **526**, 75–81 (2015).
125. Tarasov, A., Vilella, A. J., Cuppen, E., Nijman, I. J. & Prins, P. Sambamba: fast processing of NGS alignment formats. *Bioinforma. Oxf. Engl.* **31**, 2032–2034 (2015).
126. Li, H. *et al.* The Sequence Alignment/Map format and SAMtools. *Bioinforma. Oxf. Engl.* **25**, 2078–2079 (2009).
127. Mailman, M. D. *et al.* The NCBI dbGaP database of genotypes and phenotypes. *Nat. Genet.* **39**, 1181–1186 (2007).
128. Danecek, P. *et al.* Twelve years of SAMtools and BCFtools. *GigaScience* **10**, giab008 (2021).
129. Saunders, C. T. *et al.* Strelka: accurate somatic small-variant calling from sequenced tumor-normal sample pairs. *Bioinforma. Oxf. Engl.* **28**, 1811–1817 (2012).
130. Wang, K., Li, M. & Hakonarson, H. ANNOVAR: functional annotation of genetic variants from high-throughput sequencing data. *Nucleic Acids Res.* **38**, e164 (2010).
131. Xavier, A., Scott, R. J. & Talseth-Palmer, B. A. TAPES: A tool for assessment and prioritisation in exome studies. *PLoS Comput. Biol.* **15**, e1007453 (2019).
132. O'Leary, N. A. *et al.* Reference sequence (RefSeq) database at NCBI: current status, taxonomic expansion, and functional annotation. *Nucleic Acids Res.* **44**, D733-745 (2016).
133. Pedersen, B. S. & Quinlan, A. R. Mosdepth: quick coverage calculation for genomes and exomes. *Bioinforma. Oxf. Engl.* **34**, 867–868 (2018).
134. Miller, C. A., Hampton, O., Coarfa, C. & Milosavljevic, A. ReadDepth: a parallel R package for detecting copy number alterations from short sequencing reads. *PloS One* **6**, e16327 (2011).
135. Nilsen, G. *et al.* Copynumber: Efficient algorithms for single- and multi-track copy number segmentation. *BMC Genomics* **13**, 591 (2012).
136. Mermel, C. H. *et al.* GISTIC2.0 facilitates sensitive and confident localization of the targets of focal somatic copy-number alteration in human cancers. *Genome Biol.* **12**, R41 (2011).
137. Chen, X. *et al.* Manta: rapid detection of structural variants and indels for germline and cancer sequencing applications. *Bioinforma. Oxf. Engl.* **32**, 1220–1222 (2016).
138. Dobin, A. *et al.* STAR: ultrafast universal RNA-seq aligner. *Bioinforma. Oxf. Engl.* **29**, 15–21 (2013).
139. Liao, Y., Smyth, G. K. & Shi, W. featureCounts: an efficient general purpose

program for assigning sequence reads to genomic features. *Bioinforma. Oxf. Engl.* **30**, 923–930 (2014).
140. Martin, F. J. *et al.* Ensembl 2023. *Nucleic Acids Res.* **51**, D933–D941 (2023).
141. Law, C. W. *et al.* RNA-seq analysis is easy as 1-2-3 with limma, Glimma and edgeR. *F1000Research* **5**, ISCB Comm J-1408 (2016).
142. Ruel, L.-J. *et al.* Tumor Mutational Burden by Whole-Genome Sequencing in Resected NSCLC of Never Smokers. *Cancer Epidemiol. Biomark. Prev. Publ. Am. Assoc. Cancer Res. Cosponsored Am. Soc. Prev. Oncol.* **31**, 2219–2227 (2022).
143. Landrum, M. J. *et al.* ClinVar: improving access to variant interpretations and supporting evidence. *Nucleic Acids Res.* **46**, D1062–D1067 (2018).
144. Pejaver, V. *et al.* Calibration of computational tools for missense variant pathogenicity classification and ClinGen recommendations for PP3/BP4 criteria. *Am. J. Hum. Genet.* **109**, 2163–2177 (2022).
145. Sondka, Z. *et al.* The COSMIC Cancer Gene Census: describing genetic dysfunction across all human cancers. *Nat. Rev. Cancer* **18**, 696–705 (2018).
146. Wang, X. Firth logistic regression for rare variant association tests. *Front. Genet.* **5**, 187 (2014).
147. Taylor, A. M. *et al.* Genomic and Functional Approaches to Understanding Cancer Aneuploidy. *Cancer Cell* **33**, 676-689.e3 (2018).
148. Koh, G., Degasperi, A., Zou, X., Momen, S. & Nik-Zainal, S. Mutational signatures: emerging concepts, caveats and clinical applications. *Nat. Rev. Cancer* **21**, 619–637 (2021).
149. Alexandrov, L. B. *et al.* The repertoire of mutational signatures in human cancer. *Nature* **578**, 94–101 (2020).
150. Islam, S. M. A. *et al.* Uncovering novel mutational signatures by de novo extraction with SigProfilerExtractor. *Cell Genomics* **2**, None (2022).
151. Calvo, S. E., Clauser, K. R. & Mootha, V. K. MitoCarta2.0: an updated inventory of mammalian mitochondrial proteins. *Nucleic Acids Res.* **44**, D1251-1257 (2016).
152. Brady, S. W. *et al.* Pan-neuroblastoma analysis reveals age- and signature-associated driver alterations. *Nat. Commun.* **11**, 5183 (2020).
153. Choi, S. H. *et al.* Evaluation of logistic regression models and effect of covariates for case-control study in RNA-Seq analysis. *BMC Bioinformatics* **18**, 91 (2017).
154. Liao, Y., Wang, J., Jaehnig, E. J., Shi, Z. & Zhang, B. WebGestalt 2019: gene set analysis toolkit with revamped UIs and APIs. *Nucleic Acids Res.* **47**, W199–W205 (2019).
155. Karczewski, K. J. *et al.* The mutational constraint spectrum quantified from variation in 141,456 humans. *Nature* **581**, 434–443 (2020).
156. Martens, M. *et al.* WikiPathways: connecting communities. *Nucleic Acids Res.* **49**, D613–D621 (2021).
157. Pedersen, B. S. & Quinlan, A. R. Who's Who? Detecting and Resolving Sample Anomalies in Human DNA Sequencing Studies with Peddy. *Am. J. Hum. Genet.* **100**, 406–413 (2017).
158. 1000 Genomes Project Consortium *et al.* A global reference for human genetic variation. *Nature* **526**, 68–74 (2015).
159. R: The R Project for Statistical Computing. https://www.r-project.org/.
160. Heinze, G. *et al.* logistf: Firth's Bias-Reduced Logistic Regression. (2023).
161. Modeling Survival Data: Extending the Cox Model. Terry M. Therneau and Patricia M. Grambsch, Springer-Verlag, New York, 2000. No. of pages: xiii + 350. Price: $69.95. ISBN 0-387-98784-3 - Borgan - 2001 - Statistics in Medicine - Wiley Online Library. https://onlinelibrary.wiley.com/doi/10.1002/sim.956.
162. Gu, Z., Eils, R. & Schlesner, M. Complex heatmaps reveal patterns and correlations in multidimensional genomic data. *Bioinforma. Oxf. Engl.* **32**, 2847–2849 (2016).
163. Wickham, H. *Ggplot2: Elegant Graphics for Data Analysis*. (Springer, New York, NY, 2009). doi:10.1007/978-0-387-98141-3.

164. Peifer, M. *et al.* Telomerase activation by genomic rearrangements in high-risk neuroblastoma. *Nature* **526**, 700–704 (2015).
165. Bryc, K., Durand, E. Y., Macpherson, J. M., Reich, D. & Mountain, J. L. The genetic ancestry of African Americans, Latinos, and European Americans across the United States. *Am. J. Hum. Genet.* **96**, 37–53 (2015).
166. Hwang, W. L. *et al.* Clinical Impact of Tumor Mutational Burden in Neuroblastoma. *J. Natl. Cancer Inst.* **111**, 695–699 (2019).
167. Yoo, W. *et al.* A Study of Effects of MultiCollinearity in the Multivariable Analysis. *Int. J. Appl. Sci. Technol.* **4**, 9–19 (2014).
168. Chen, Y. *et al.* Oncogenic mutations of ALK kinase in neuroblastoma. *Nature* **455**, 971–974 (2008).
169. Valencia-Sama, I. *et al.* NRAS Status Determines Sensitivity to SHP2 Inhibitor Combination Therapies Targeting the RAS-MAPK Pathway in Neuroblastoma. *Cancer Res.* **80**, 3413–3423 (2020).
170. Cimmino, F. *et al.* FGFR1 is a potential therapeutic target in neuroblastoma. *Cancer Cell Int.* **22**, 174 (2022).
171. Nunes-Xavier, C. E. *et al.* Protein Tyrosine Phosphatases in Neuroblastoma: Emerging Roles as Biomarkers and Therapeutic Targets. *Front. Cell Dev. Biol.* **9**, 811297 (2021).
172. Wang, H., Wang, X., Xu, L. & Zhang, J. TP53 and TP53-associated genes are correlated with the prognosis of paediatric neuroblastoma. *BMC Genomic Data* **23**, 41 (2022).
173. Wang, Y., Liu, S., Zhang, Y. & Yang, J. Myosin Heavy Chain 9: Oncogene or Tumor Suppressor Gene? *Med. Sci. Monit. Int. Med. J. Exp. Clin. Res.* **25**, 888–892 (2019).
174. Liao, H.-Y., Da, C.-M., Wu, Z.-L. & Zhang, H.-H. Ski: Double roles in cancers. *Clin. Biochem.* **87**, 1–12 (2021).
175. Shao, J.-B., Gao, Z.-M., Huang, W.-Y. & Lu, Z.-B. The mechanism of epithelial-mesenchymal transition induced by TGF-β1 in neuroblastoma cells. *Int. J. Oncol.* **50**, 1623–1633 (2017).
176. Lovén, J. *et al.* MYCN-regulated microRNAs repress estrogen receptor-alpha (ESR1) expression and neuronal differentiation in human neuroblastoma. *Proc. Natl. Acad. Sci. U. S. A.* **107**, 1553–1558 (2010).
177. Ichimiya, S. *et al.* p73 at chromosome 1p36.3 is lost in advanced stage neuroblastoma but its mutation is infrequent. *Oncogene* **18**, 1061–1066 (1999).
178. Depuydt, P. *et al.* Meta-mining of copy number profiles of high-risk neuroblastoma tumors. *Sci. Data* **5**, 180240 (2018).
179. Janoueix-Lerosey, I. *et al.* Overall genomic pattern is a predictor of outcome in neuroblastoma. *J. Clin. Oncol. Off. J. Am. Soc. Clin. Oncol.* **27**, 1026–1033 (2009).
180. Lee, C. H., Cook, S., Lee, J. S. & Han, B. Comparison of Two Meta-Analysis Methods: Inverse-Variance-Weighted Average and Weighted Sum of Z-Scores. *Genomics Inform.* **14**, 173–180 (2016).
181. Cunsolo, C. L., Bicocchi, M. P., Petti, A. R. & Tonini, G. P. Numerical and structural aberrations in advanced neuroblastoma tumours by CGH analysis; survival correlates with chromosome 17 status. *Br. J. Cancer* **83**, 1295–1300 (2000).
182. Mosse, Y. P. *et al.* Neuroblastomas have distinct genomic DNA profiles that predict clinical phenotype and regional gene expression. *Genes. Chromosomes Cancer* **46**, 936–949 (2007).
183. Michels, E. *et al.* ArrayCGH-based classification of neuroblastoma into genomic subgroups. *Genes. Chromosomes Cancer* **46**, 1098–1108 (2007).
184. Caron, H. *et al.* Allelic loss of chromosome 1p as a predictor of unfavorable outcome in patients with neuroblastoma. *N. Engl. J. Med.* **334**, 225–230 (1996).
185. Bilke, S., Chen, Q.-R., Wei, J. S. & Khan, J. Whole chromosome alterations predict survival in high-risk neuroblastoma without MYCN amplification. *Clin. Cancer Res. Off.*

J. Am. Assoc. Cancer Res. **14**, 5540–5547 (2008).
186. Savelyeva, L., Corvi, R. & Schwab, M. Translocation involving 1p and 17q is a recurrent genetic alteration of human neuroblastoma cells. *Am. J. Hum. Genet.* **55**, 334–340 (1994).
187. Sheng, M. & Sala, C. PDZ domains and the organization of supramolecular complexes. *Annu. Rev. Neurosci.* **24**, 1–29 (2001).
188. Boeckers, T. M., Bockmann, J., Kreutz, M. R. & Gundelfinger, E. D. ProSAP/Shank proteins - a family of higher order organizing molecules of the postsynaptic density with an emerging role in human neurological disease. *J. Neurochem.* **81**, 903–910 (2002).
189. Griesius, S. *et al.* Reduced expression of the psychiatric risk gene DLG2 (PSD93) impairs hippocampal synaptic integration and plasticity. *Neuropsychopharmacol. Off. Publ. Am. Coll. Neuropsychopharmacol.* **47**, 1367–1378 (2022).
190. Sanders, B. *et al.* Transcriptional programs regulating neuronal differentiation are disrupted in DLG2 knockout human embryonic stem cells and enriched for schizophrenia and related disorders risk variants. *Nat. Commun.* **13**, 27 (2022).
191. Shao, Y. W. *et al.* Cross-species genomics identifies DLG2 as a tumor suppressor in osteosarcoma. *Oncogene* **38**, 291–298 (2019).
192. Gründer, S. & Chen, X. Structure, function, and pharmacology of acid-sensing ion channels (ASICs): focus on ASIC1a. *Int. J. Physiol. Pathophysiol. Pharmacol.* **2**, 73–94 (2010).
193. Huang, Y. *et al.* Two aspects of ASIC function: Synaptic plasticity and neuronal injury. *Neuropharmacology* **94**, 42–48 (2015).
194. Sivils, A., Yang, F., Wang, J. Q. & Chu, X.-P. Acid-Sensing Ion Channel 2: Function and Modulation. *Membranes* **12**, 113 (2022).
195. Zhou, Z.-H. *et al.* The acid-sensing ion channel, ASIC2, promotes invasion and metastasis of colorectal cancer under acidosis by activating the calcineurin/NFAT1 axis. *J. Exp. Clin. Cancer Res. CR* **36**, 130 (2017).
196. Meng, C. *et al.* IKZF3 modulates cerebral ischemia/reperfusion injury by inhibiting neuroinflammation. *Int. Immunopharmacol.* **114**, 109480 (2023).
197. Yang, L.-K. *et al.* Novel IKZF3 transcriptomic signature correlates with positive outcomes of skin cutaneous melanoma: A pan-cancer analysis. *Front. Genet.* **13**, 1036402 (2022).
198. Maguire, L. H., Thomas, A. R. & Goldstein, A. M. Tumors of the neural crest: Common themes in development and cancer. *Dev. Dyn. Off. Publ. Am. Assoc. Anat.* **244**, 311–322 (2015).
199. Shen, Z. Genomic instability and cancer: an introduction. *J. Mol. Cell Biol.* **3**, 1–3 (2011).
200. Knijnenburg, T. A. *et al.* Genomic and Molecular Landscape of DNA Damage Repair Deficiency across The Cancer Genome Atlas. *Cell Rep.* **23**, 239-254.e6 (2018).
201. Degasperi, A. *et al.* Substitution mutational signatures in whole-genome-sequenced cancers in the UK population. *Science* **376**, science.abl9283 (2022).
202. Huang, R.-X. & Zhou, P.-K. DNA damage response signaling pathways and targets for radiotherapy sensitization in cancer. *Signal Transduct. Target. Ther.* **5**, 60 (2020).
203. Jewell, R. *et al.* Patterns of expression of DNA repair genes and relapse from melanoma. *Clin. Cancer Res. Off. J. Am. Assoc. Cancer Res.* **16**, 5211–5221 (2010).
204. Park, S. *et al.* Comprehensive DNA repair gene expression analysis and its prognostic significance in acute myeloid leukemia. *Hematol. Amst. Neth.* **26**, 904–913 (2021).
205. Mohamed, R. I. *et al.* The overexpression of DNA repair genes in invasive ductal and lobular breast carcinomas: Insights on individual variations and precision medicine. *PloS One* **16**, e0247837 (2021).
206. Kimura, S. *et al.* Association of high-risk neuroblastoma classification based on

expression profiles with differentiation and metabolism. *PloS One* **16**, e0245526 (2021).
207. Richards, S. *et al.* Standards and guidelines for the interpretation of sequence variants: a joint consensus recommendation of the American College of Medical Genetics and Genomics and the Association for Molecular Pathology. *Genet. Med. Off. J. Am. Coll. Med. Genet.* **17**, 405–424 (2015).
208. Conforti, F. *et al.* Biological and clinical features of triple negative Invasive Lobular Carcinomas of the breast. Clinical outcome and actionable molecular alterations. *Breast Edinb. Scotl.* **59**, 94–101 (2021).
209. Winckers, L. A., Evelo, C. T., Willighagen, E. L. & Kutmon, M. Investigating the Molecular Processes behind the Cell-Specific Toxicity Response to Titanium Dioxide Nanobelts. *Int. J. Mol. Sci.* **22**, 9432 (2021).
210. Turk, A. & Kunej, T. Shared Genetic Risk Factors Between Cancer and Cardiovascular Diseases. *Front. Cardiovasc. Med.* **9**, 931917 (2022).
211. Toh, M. & Ngeow, J. Homologous Recombination Deficiency: Cancer Predispositions and Treatment Implications. *The Oncologist* **26**, e1526–e1537 (2021).
212. Jian, X., Boerwinkle, E. & Liu, X. In silico prediction of splice-altering single nucleotide variants in the human genome. *Nucleic Acids Res.* **42**, 13534–13544 (2014).
213. Körber, V. *et al.* Neuroblastoma arises in early fetal development and its evolutionary duration predicts outcome. *Nat. Genet.* **55**, 619–630 (2023).
214. Mu, Y. *et al.* Identification of stromal differentially expressed proteins in the colon carcinoma by quantitative proteomics. *Electrophoresis* **34**, 1679–1692 (2013).
215. Schramek, D. *et al.* Direct in vivo RNAi screen unveils myosin IIa as a tumor suppressor of squamous cell carcinomas. *Science* **343**, 309–313 (2014).
216. Zhao, B. *et al.* The non-muscle-myosin-II heavy chain Myh9 mediates colitis-induced epithelium injury by restricting Lgr5+ stem cells. *Nat. Commun.* **6**, 7166 (2015).
217. Massagué, J. TGFbeta in Cancer. *Cell* **134**, 215–230 (2008).
218. Fetahu, I. S. & Taschner-Mandl, S. Neuroblastoma and the epigenome. *Cancer Metastasis Rev.* **40**, 173–189 (2021).
219. Gautier, M., Thirant, C., Delattre, O. & Janoueix-Lerosey, I. Plasticity in Neuroblastoma Cell Identity Defines a Noradrenergic-to-Mesenchymal Transition (NMT). *Cancers* **13**, 2904 (2021).
220. Ho, N. *et al.* Delineation of the frequency and boundary of chromosomal copy number variations in paediatric neuroblastoma. *Cell Cycle Georget. Tex* **17**, 749–758 (2018).
221. Irwin, M. S. *et al.* Revised Neuroblastoma Risk Classification System: A Report From the Children's Oncology Group. *J. Clin. Oncol. Off. J. Am. Soc. Clin. Oncol.* **39**, 3229–3241 (2021).
222. Oppedal, B. R., Storm-Mathisen, I., Lie, S. O. & Brandtzaeg, P. Prognostic factors in neuroblastoma. Clinical, histopathologic, and immunohistochemical features and DNA ploidy in relation to prognosis. *Cancer* **62**, 772–780 (1988).
223. Look, A. T., Hayes, F. A., Nitschke, R., McWilliams, N. B. & Green, A. A. Cellular DNA content as a predictor of response to chemotherapy in infants with unresectable neuroblastoma. *N. Engl. J. Med.* **311**, 231–235 (1984).
224. Fransson, S. *et al.* Whole-genome sequencing of recurrent neuroblastoma reveals somatic mutations that affect key players in cancer progression and telomere maintenance. *Sci. Rep.* **10**, 22432 (2020).
225. Zanon, C. & Tonini, G. P. Transcription instability in high-risk neuroblastoma is associated with a global perturbation of chromatin domains. *Mol. Oncol.* **11**, 1646–1658 (2017).
226. Pilati, C. *et al.* Mutational signature analysis identifies MUTYH deficiency in colorectal cancers and adrenocortical carcinomas. *J. Pathol.* **242**, 10–15 (2017).
227. Alexandrov, L. B., Nik-Zainal, S., Wedge, D. C., Campbell, P. J. & Stratton, M. R. Deciphering signatures of mutational processes operative in human cancer. *Cell Rep.* **3**,

246–259 (2013).
228. Rowe, L. A., Degtyareva, N. & Doetsch, P. W. DNA damage-induced reactive oxygen species (ROS) stress response in Saccharomyces cerevisiae. *Free Radic. Biol. Med.* **45**, 1167–1177 (2008).
229. Kiwerska, K. & Szyfter, K. DNA repair in cancer initiation, progression, and therapy-a double-edged sword. *J. Appl. Genet.* **60**, 329–334 (2019).
230. O'Neil, N. J., Bailey, M. L. & Hieter, P. Synthetic lethality and cancer. *Nat. Rev. Genet.* **18**, 613–623 (2017).
231. Zeineldin, M., Patel, A. G. & Dyer, M. A. Neuroblastoma: When differentiation goes awry. *Neuron* **110**, 2916–2928 (2022).
232. Boultwood, J. Ataxia telangiectasia gene mutations in leukaemia and lymphoma. *J. Clin. Pathol.* **54**, 512–516 (2001).
233. Cybulski, C. *et al.* CHEK2 is a multiorgan cancer susceptibility gene. *Am. J. Hum. Genet.* **75**, 1131–1135 (2004).
234. Yamamoto, H. & Hirasawa, A. Homologous Recombination Deficiencies and Hereditary Tumors. *Int. J. Mol. Sci.* **23**, 348 (2021).